Redox Biology 51 (2022) 102261

Contents lists available at ScienceDirect

Redox Biology

journal homepage: www.elsevier.com/locate/redox

REV-ERBα regulates age-related and oxidative stress-induced degeneration in retinal pigment epithelium via NRF2

Shuo Huang [a,1], Chi-Hsiu Liu [a,1], Zhongxiao Wang [a], Zhongjie Fu [a], William R. Britton [a], Alexandra K. Blomfield [a], Theodore M. Kamenecka [b], Joshua L. Dunaief [c], Laura A. Solt [d,b], Jing Chen [a,*]

[a] Department of Ophthalmology, Boston Children's Hospital, Harvard Medical School, 300 Longwood Avenue, Boston, MA, 02115, USA
[b] Department of Molecular Medicine, The Scripps Research Institute, 130 Scripps Way, Jupiter, FL, 33458, USA
[c] F.M. Kirby Center for Molecular Ophthalmology, Scheie Eye Institute, Perelman School of Medicine at the University of Pennsylvania, 305 Stellar-Chance Laboratory, 422 Curie Blvd, Philadelphia, PA, 19104, USA
[d] Department of Immunology and Microbiology, The Scripps Research Institute, 130 Scripps Way, Jupiter, FL, 33458, USA

ARTICLE INFO

Keywords:
Retinal pigment epithelium
Aging
Age-related macular degeneration
REV-ERBα
Oxidative damage
NRF2

ABSTRACT

Retinal pigment epithelium (RPE) dysfunction and atrophy occur in dry age-related macular degeneration (AMD), often leading to photoreceptor degeneration and vision loss. Accumulated oxidative stress during aging contributes to RPE dysfunction and degeneration. Here we show that the nuclear receptor REV-ERBα, a redox sensitive transcription factor, protects RPE from age-related degeneration and oxidative stress-induced damage. Genetic deficiency of REV-ERBα leads to accumulated oxidative stress, dysfunction and degeneration of RPE, and AMD-like ocular pathologies in aging mice. Loss of REV-ERBα exacerbates chemical-induced RPE damage, and pharmacological activation of REV-ERBα protects RPE from oxidative damage both *in vivo* and *in vitro*. REV-ERBα directly regulates transcription of nuclear factor erythroid 2-related factor 2 (NRF2) and its downstream antioxidant enzymes superoxide dismutase 1 (SOD1) and catalase to counter oxidative damage. Moreover, aged mice with RPE specific knockout of REV-ERBα also exhibit accumulated oxidative stress and fundus and RPE pathologies. Together, our results suggest that REV-ERBα is a novel intrinsic protector of the RPE against age-dependent oxidative stress and a new molecular target for developing potential therapies to treat age-related retinal degeneration.

1. Introduction

Age-related macular degeneration (AMD) is a major cause of irreversible blindness in the elderly impacting over 2 million seniors in the US alone, and the number is expected to increase worldwide with the aging population [1–3]. Advanced AMD includes the neovascular form (wet) and the more common dry form, with latter accounting for about 90% cases of AMD. Dry AMD onset is characterized by dysfunctional retinal pigment epithelium (RPE) cells and focal deposition of lipid-enriched drusen (hallmark of AMD) between the RPE layer and Bruch's membrane [1,2]. The RPE, a thin layer of epithelial cells behind the retina, functions mainly to renew photoreceptor outer segments via phagocytosis and to recycle visual pigments, thereby providing trophic support for photoreceptors. Dysfunction of the RPE can lead to accumulated cell debris and metabolic waste, resulting in a thickened Bruch's membrane, formation of drusen and subretinal drusenoid deposits (pseudo-drusen) [1,2,4–6]. Photoreceptor degeneration thereby occurs, thus leading to visual impairment [7]. Although RPE cells diminish in number even with normal aging, these cells degenerate more rapidly in advanced dry AMD (known as geographic atrophy). Currently there is no treatment to stop or slow RPE degeneration in AMD. Discovering new therapies to preserve RPE health is critical for AMD prevention and treatment.

AMD has both environmental and genetic risk factors [8], including smoking, and genetic variations in antioxidant enzymes in a small cohort [9], both of which are linked with increased oxidative stress. Oxidative stress plays a substantive role in AMD development due to high oxygen consumption, photo-oxidation, and lipid radicals, all of

* Corresponding author.
E-mail address: jing.chen@childrens.harvard.edu (J. Chen).
[1] These authors contributed equally to this work.

https://doi.org/10.1016/j.redox.2022.102261
Received 30 November 2021; Received in revised form 2 February 2022; Accepted 5 February 2022
Available online 9 February 2022

which contribute to high levels of oxidative stress surrounding the retina [10,11]. The oxidative homeostasis in the retina and RPE is normally maintained by the presence of efficient antioxidants and repair systems, with nuclear factor erythroid 2-related factor 2 (NRF2) as a master transcriptional regulator of endogenous antioxidant and phase II detoxification enzymes [12,13]. Upon activation, NRF2 induces the production of antioxidant enzymes such as catalase and superoxide dismutase (SOD), as well as phase II detoxification enzymes such as glutathione s-transferases [14]. NRF2 was established as an essential cytoprotective signaling system in RPE aging and AMD in both clinical and experimental studies. In clinical AMD specimens, NRF2 was decreased in dysmorphic RPE cells overlaying drusen [15]. C57BL/6J mice exposed to cigarette smoke over time have marked RPE degeneration with impaired NRF2 signaling [15,16]. In addition, NRF2 deficient mice develop age-related retinal pathology [17]. The potential of promoting antioxidant defense in AMD management is further supported by findings from AREDS/AREDS2 (Age-Related Eye Disease Studies), which showed the protective effects of antioxidant vitamins in slowing AMD progression [18].

Nuclear receptors have been increasingly recognized as novel regulators of retinal and RPE health, and can be targeted for their therapeutic potential [19,20]. A nuclear receptor atlas identified that the orphan nuclear receptor REV-ERBα is expressed in high levels in freshly isolated human RPE cells [21]. REV-ERBα, a reduction/oxidation (redox)-sensitive transcription factor, is highly expressed in the liver, adipose tissue, skeletal muscle, and brain, where it is transcribed and translated in a circadian manner and regulates many biological processes including circadian rhythm, lipid and glucose metabolism, macrophage inflammatory response, mitochondrial biosynthesis and autoimmune function [22–34]. The transcriptional regulatory function of REV-ERBα is activated upon binding with its ligand heme [35]. REV-ERBα can form a potent transcriptional repressor complex with corepressor proteins, typically the nuclear receptor co-repressor-1 (NCoR1) and the histone deacetylase 3 (HDAC3) [35,36]; together the complex can bind to specific ROR response elements (RORE/RevRE) in the regulatory regions of target genes to repress their transcription [23,27,37], such as brain and muscle ARNT-like 1 (BMAL1) [23] and circadian locomotor output cycles protein kaput (CLOCK) [38]. Besides, a dual role of REV-ERBα as a transcriptional activator has also been reported for some of its target genes [31], including genes involved in retinal development [26,39]. However, the potential role of REV-ERBα in the eye and particularly RPE health and disease remains understudied.

In this study we investigated the role of REV-ERBα in RPE function and health in two models of aging-induced degeneration and chemical-induced oxidative damage. Here we provide evidence that REV-ERBα is an endogenous protector of RPE health during aging, and that it augments antioxidant defense in the RPE through transcriptional regulation of NRF2 and its target enzymes. Our data demonstrate that genetic deficiency of REV-ERBα in mice causes fundus lesions and RPE dysfunction and atrophy during aging, associated with increased oxidative stress in the eye. Genetic loss of REV-ERBα exacerbates oxidative stress-induced RPE damage and pharmacological activation of REV-ERBα protects the RPE in an acute model of chemical-induced oxidative damage. REV-ERBα directly activates NRF2 transcription and upregulates the expression of its downstream antioxidant enzymes, to promote RPE self-defense. Our work builds on the discovery of REV-ERBα as a key factor regulating RPE function and survival and suggests that modulation of REV-ERBα may serve as a novel therapeutic method to promote RPE health and survival in AMD.

2. Results

2.1. REV-ERBα is localized in the RPE and retinas in mice

We first sought to determine the expression profile of REV-ERBα in the RPE of mouse eyes during aging. Immunohistochemical staining of wild-type (WT) mouse eyes showed that REV-ERBα co-localized with DAPI in RPE nuclei (Fig. 1A), expected as a nuclear receptor. Moreover, REV-ERBα protein levels in RPE decline with age, with approximately 25% of decline at 7–8 months old, and around 35% of decline by 10–11 months old, compared with 2–3 months old, indicating that gradual loss of REV-ERBα may potentially be involved in RPE aging (Fig. 1B and C). Localization of REV-ERBα is also found in retinal neurons including photoreceptors, inner nuclear layer and ganglion cell layer with immunohistochemistry (Fig. S1A).

2.2. REV-ERBα deficiency leads to sub-retinal lipid-enriched deposits

To investigate the function of REV-ERBα in the eye, we first performed ocular funduscopic examination of age-matched *Rev-erbα*$^{+/+}$ and *Rev-erbα*$^{-/-}$ mice at 3, 6, and 12 months old. Fundus imaging from *Rev-erbα*$^{-/-}$ mice revealed abnormal bilateral whitish-yellow-colored sub-retinal lesions, starting with sporadic lesions at 3 months old (Fig. 1D). Prevalence of these lesions increased substantially with age in *Rev-erbα*$^{-/-}$ mice: at 6 months old the number of lesions were about 4-fold higher compared with age-matched *Rev-erbα*$^{+/+}$ mice and at 12 months old the lesion numbers in *Rev-erbα*$^{-/-}$ mice was 3-fold higher than age-matched *Rev-erbα*$^{+/+}$ mice (Fig. 1E). Fundus imaging also exhibits lesions with autofluorescence (AF) (Fig. S1B). Moreover, accumulation of oil red O-positive lipid-enriched sub-retinal deposits were observed in the *Rev-erbα*$^{-/-}$ eyes starting at 5 months old, and became more frequent at 12 months old. Lipid-enriched deposits of a significantly large size were occasionally detected in 12-month-old *Rev-erbα*$^{-/-}$ eyes (Fig. 1F), reflecting potential disrupted spent outer segment recycle and phagocytosis by RPE.

2.3. Loss of REV-ERBα results in RPE degeneration in mice

To examine the integrity of the *Rev-erbα*$^{-/-}$ RPE, immunohistochemical staining of β-catenin and DAPI was performed on RPE/choroid flat mounts. *Rev-erbα*$^{-/-}$ RPEs showed patchy areas of atrophy with partial or complete disruption of cellular adherent junctions (stained with β-catenin, green) and substantial nuclear fragmentation (stained in DAPI, blue) at 12 months old, whereas age-matched *Rev-erbα*$^{+/+}$ RPEs were normal with intact nuclei (Fig. 2A). Interestingly, when the RPE/choroid flat mounts of 12-month-old WT and *Rev-erbα*$^{-/-}$ mice were stained with the tight junction marker ZO-1, there was no obvious loss of RPE tight junctions in REV-ERBα-deficient mice; however, these *Rev-erbα*$^{-/-}$ mice exhibited a significantly greater number of abnormal RPE cells with shrunken (<200 μm^2) or enlarged (>500 μm^2) cell size, and fewer RPE cells within normal size range (200–500 μm^2) (Fig. S2). Both increased RPE nuclear fragmentation and abnormal and increased cell size in *Rev-erbα*$^{-/-}$ mice are suggestive of accelerated RPE aging [40]. At 16 months old, *Rev-erbα*$^{-/-}$ eyes showed areas of prominent RPE disorganization with very non-uniform morphology in shape and pigmentation, with disrupted RPE in toluidine blue staining of epoxy semi-thin sections (Fig. 2B). Similarly discontinued RPE was observed in 12- and 18-month-old *Rev-erbα*$^{-/-}$ eye sections with H&E staining (Fig. S3).

To further investigate if *Rev-erbα*$^{-/-}$ mice develop drusen-like deposits in the sub-retinal area, we conducted immunohistochemical staining using two drusen component markers: vitronectin, an extracellular matrix protein [41], and C3, a complement system component [5]. In *Rev-erbα*$^{-/-}$ mice, both vitronectin and C3 antibodies demonstrated significantly increased staining intensity in the sub-RPE areas around Bruch's membrane (BrM) (Fig. 2C), and drusen-like structure were observed (Fig. 2C). Protein levels of C3 were enriched in *Rev-erbα*$^{-/-}$ RPEs compared with *Rev-erbα*$^{+/+}$ RPEs as detected with Western blotting (Fig. 2D). Frequency analysis of age-related RPE pathologies was performed in *Rev-erbα*$^{+/+}$ and *Rev-erbα*$^{-/-}$ eyes (Fig. S3) and is summarized in Table 1, showing higher number of *Rev-erbα*$^{-/-}$ eyes with RPE hypopigmentation and hyperpigmentation, as well as

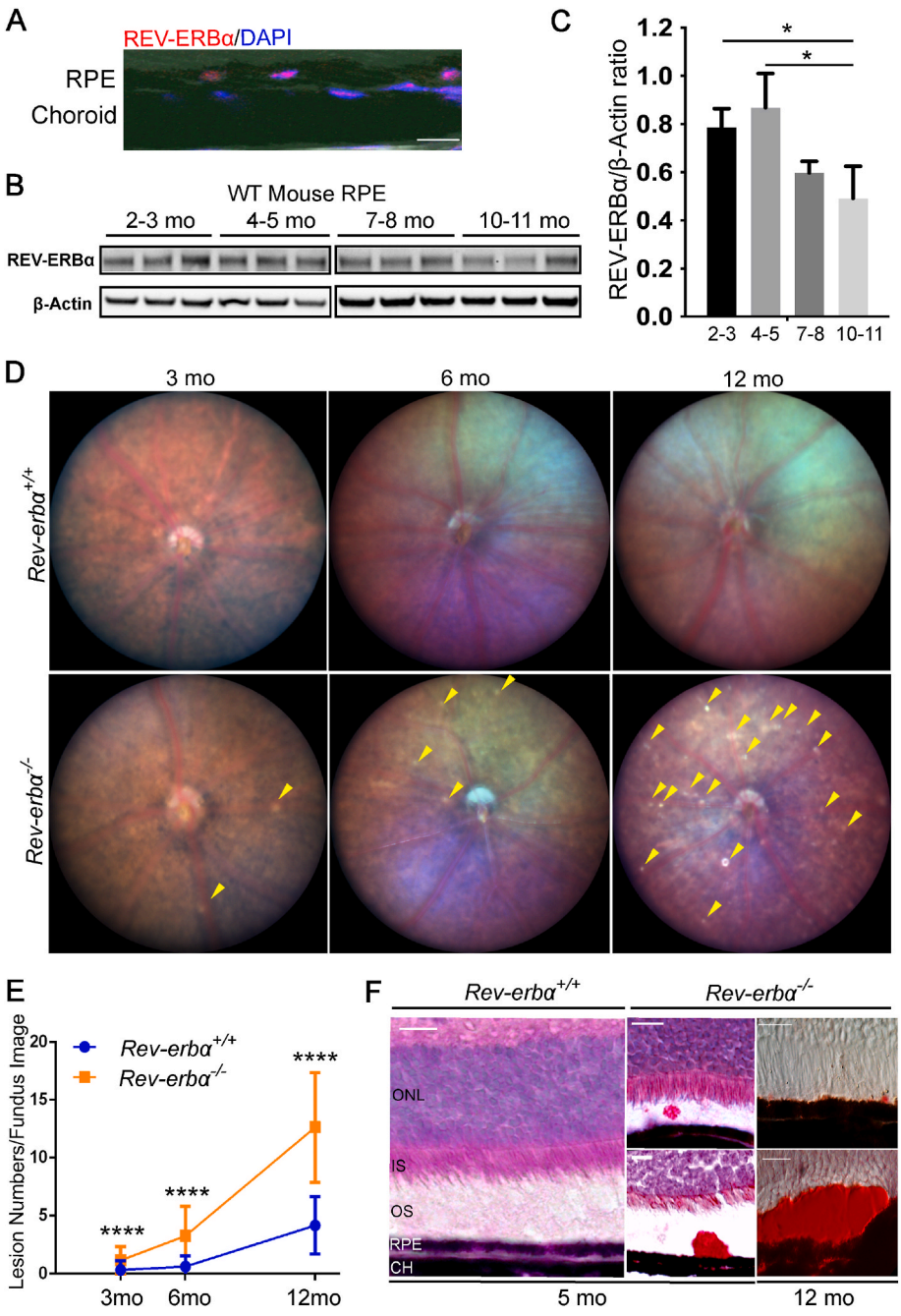

Fig. 1. REV-ERBα declines in aging RPE and sub-retinal deposits increase in *Rev-erbα*$^{-/-}$ mice. (A) Immunostaining of cross-sections from Wild-type (WT) mice shows REV-ERBα antibody staining (red) in RPE nuclei, co-localized with nucleus marker DAPI (blue). Scale bar: 10 μm. (B–C) Western blot (B) and quantification (C) of REV-ERBα protein levels in the RPE isolated from 2–3, 4–5, 7–8 and 10–11 months old WT mice. Protein size: REV-ERBα (67 kDa), β-Actin (42 kDa). n = 3 mice/group. Quantification statistics was performed with nonparametric Kruskal-Wallis test. (D) *Rev-erbα*$^{-/-}$ retinas show an increasing number of whitish abnormal deposits (yellow arrowheads) in fundus imaging with aging at 3, 6, and 12 months old (n = 10–12 eyes from 5 to 6 mice/group, mixed genders). (E) Quantification of the total lesion numbers in fundus images of *Rev-erbα*$^{+/+}$and *Rev-erbα*$^{-/-}$ mice during aging (n = 10–12 eyes/group). (F) *Rev-erbα*$^{-/-}$ retinas show oil red O-positive staining (red) as lipid marker in the sub-retinal deposits (red), which are counter-stained with hematoxylin in 5-month-old eyes; in 12-month-old eyes sub-retinal deposits are stained with oil red O only. Scale bar: 20 μm. Error bars indicate SD. *: $P < 0.05$; ****: $P < 0.0001$. (For interpretation of the references to color in this figure legend, the reader is referred to the Web version of this article.)

drusen-like deposit vs. *Rev-erbα*$^{+/+}$ eyes.

The development of sub-retinal deposits in *Rev-erbα*$^{-/-}$ eyes was further confirmed in electron microscopy (EM) analysis of 6-month-old mice. Quantification of the overall thickness of BrM indicated significantly thickened BrM (~2 fold) in *Rev-erbα*$^{-/-}$ eyes at 6 months old compared with *Rev-erbα*$^{+/+}$ eyes (Fig. 2E). This quantification excludes extensively thickened outer collagenous layers (OCL) within BrM observed in certain sub-RPE areas of *Rev-erbα*$^{-/-}$ eyes. Furthermore, at 18 months old, significant focal RPE degeneration was observed in *Rev-erbα*$^{-/-}$ eyes with RPE vacuolization and loss and disorganization of nearby photoreceptor outer segments (Fig. 2F), whereas age-matched *Rev-erbα*$^{+/+}$ mice had normal RPE and intact photoreceptor outer segments. These data suggest that loss of REV-ERBα accelerates RPE aging and results in early RPE atrophy and abnormal sub-retinal deposits in mice.

2.4. Genetic deficiency of REV-ERBα decreases RPE phagocytic activity

RPE cells function primarily to remove distal photoreceptor outer segments (POS) tips by receptor-mediated phagocytosis, a process that peaks in the morning (1–2 h after the onset of light) [42]. RPE isolated from AMD vs. normal donors have significantly reduced RPE phagocytosis activity, which normally declines with age only moderately [43]. To investigate if REV-ERBα deficiency impacts RPE phagocytosis function, RPE phagocytic activity was analyzed *in situ* in 6-month-old *Rev-erbα*$^{+/+}$ and *Rev-erbα*$^{-/-}$ mice. Uptake of cone outer segments was measured by staining of rhodamine labeled peanut agglutinin (PNA) [44] in phalloidin-delineated RPE flat mounts, and was dramatically decreased by ~3 fold in the *Rev-erbα*$^{-/-}$ mice *in vivo* (Fig. 3A and B), suggesting severely impaired RPE phagocytosis in *Rev-erbα*$^{-/-}$ eyes.

To corroborate the *in vivo* findings, primary RPE cells were isolated from 2-month-old *Rev-erbα*$^{+/+}$ and *Rev-erbα*$^{-/-}$ mice and cultured to

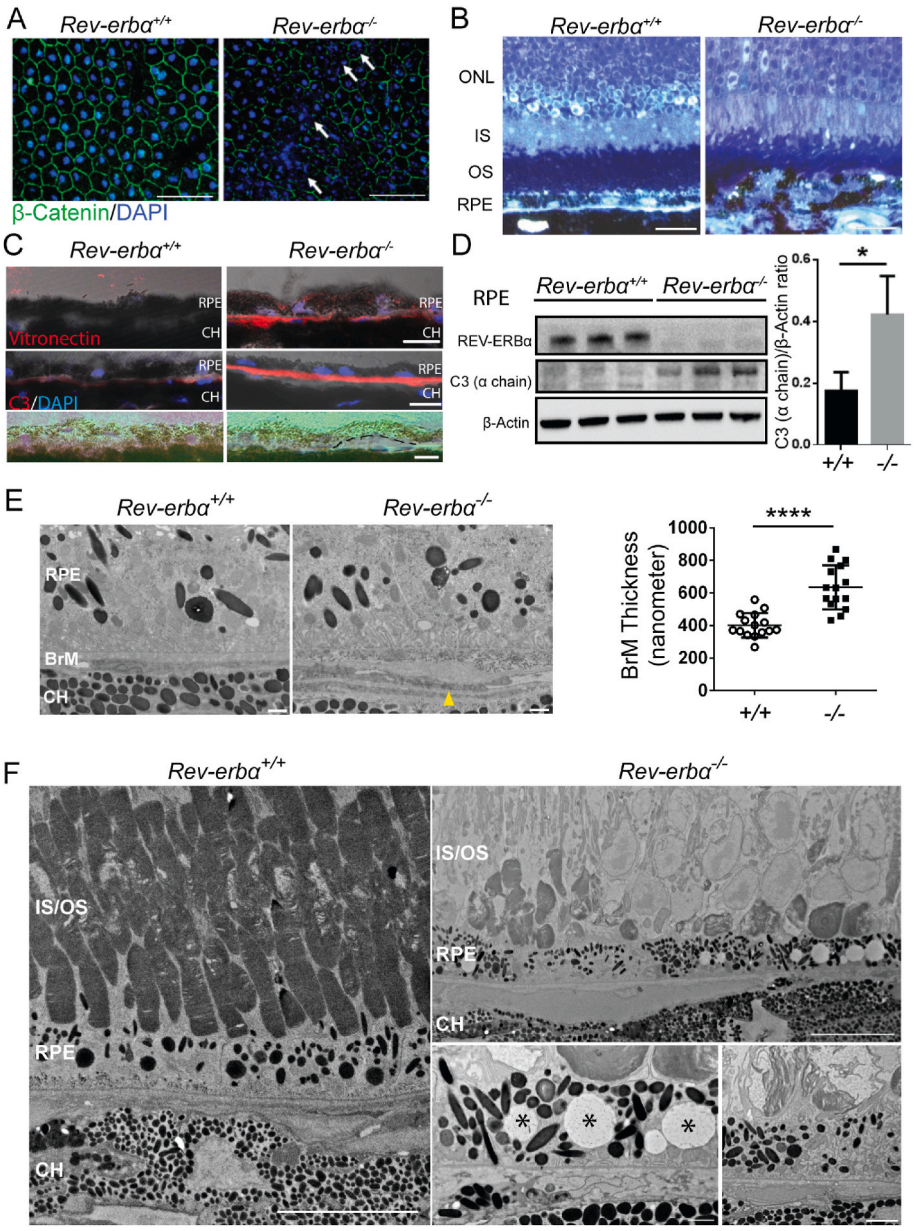

Fig. 2. RPE degeneration in *Rev-erbα*$^{-/-}$ eyes. (A) Isolated RPE/choroid complex flat mounts from 12-month-old *Rev-erbα*$^{+/+}$ and *Rev-erbα*$^{-/-}$ mice stained with β-catenin (green) and DAPI (blue). White arrows indicate areas with junctional disruption and nuclear fragmentation. Scale bar: 50 μm. (B) Toluidine blue staining of epoxy semi-thin sections of *Rev-erbα*$^{+/+}$ and *Rev-erbα*$^{-/-}$ eyes from 16-month-old mice. Scale bar: 20 μm. (C) Increased sub-RPE deposition of vitronectin and C3 in *Rev-erbα*$^{-/-}$ vs. *Rev-erbα*$^{+/+}$ eyes at 16 months old. Drusen-like deposit (highlighted by black dash line) are shown in *Rev-erbα*$^{-/-}$ but not *Rev-erbα*$^{+/+}$ eyes at 12 months old. Scale bar: 10 μm. (D) Western blot and quantification show higher C3 (α chain) protein levels in *Rev-erbα*$^{-/-}$ RPE in 12-month-old mice compared with age-matched *Rev-erbα*$^{+/+}$ mice. Protein size: C3 α chain (115 kDa). n = 3 mice/group. (E) Electron microscopy (EM) imaging of 6-month-old *Rev-erbα*$^{-/-}$ mice show outer collagenous (OCL) deposits (indicated by yellow arrowhead) in Bruch's membrane (BrM) and increased BrM thickness compared with WT as quantified. Scale bar: 1 μm. (F) EM images from 18-month-old *Rev-erbα*$^{-/-}$ eyes show focal loss of photoreceptor outer segments (upper panel, scale bar, 10 μm), vacuolization in the RPE (bottom left panel, marked by asterisks, scale bar, 1 μm), and disorganized outer segment disc membranous material surrounded by the microvilli of the RPE (bottom right panel scale bar, 2 μm), compared with age-matched WT eyes (left panel, scale bar: 10 μm). Error bars indicate SD. *: $P < 0.05$, ****: $P < 0.0001$. (For interpretation of the references to color in this figure legend, the reader is referred to the Web version of this article.)

Table 1
Summary of histological analysis of RPE degeneration in *Rev-erbα*$^{+/+}$ and *Rev-erbα*$^{-/-}$ mice (incidences/eyes examined).

Rev-erbα$^{+/+}$ eyes		RPE pathology		
Age (month)	Number of eyes	Hyperpigmentation	Hypopigmentation	Drusen-like deposit
5–6	5	0/5	0/5	0/5
12–13	8	1/8	0/8	0/8
17–18	8	3/8	2/8	0/8
Rev-erbα$^{-/-}$ eyes		RPE pathology		
Age (month)	Number of eyes	Hyperpigmentation	Hypopigmentation	Drusen-like deposit
5–6	10	3/10	2/10	0/10
12–13	17	16/17	8/17	2/17
17–18	9	9/9	9/9	1/9

assess their phagocytic function of ingesting porcine POS. Primary *Rev-erbα*$^{-/-}$ RPE cells consistently demonstrated ~70% fewer ingested fluorescent-tagged POS compared to primary *Rev-erbα*$^{+/+}$ cells (Fig. 3C and D). RPE phagocytic processes comprise three distinct phases: recognition and binding, internalization, and digestion, each of which is distinctly regulated [45]. The reduced number of POS in RPE cells suggests either dampened internalization or more rapid digestion of POS in the cells. Next, we fed the cultured mouse primary RPE cells microspheres, which can be engulfed by the cells but cannot be digested in lysosomes, to delineate the endocytosis process [46]. *Rev-erbα*$^{-/-}$ RPE

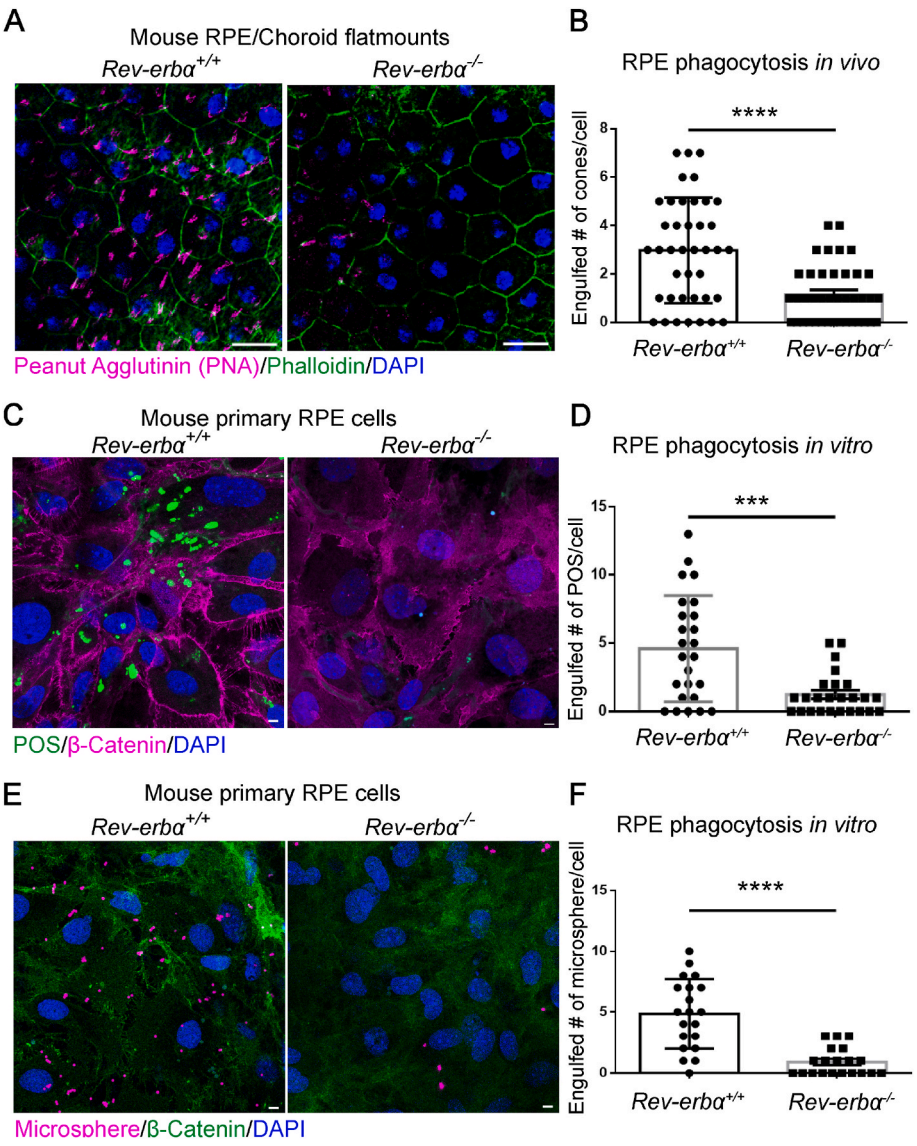

Fig. 3. REV-ERBα deficiency decreases RPE phagocytic activity. (A) RPE/choroid flat mounts from 6-month-old *Rev-erbα*$^{+/+}$ and *Rev-erbα*$^{-/-}$ mice were stained with peanut agglutinin (magenta), phalloidin (green) and DAPI (blue). Scale bar: 20 μm. (B) Quantification of engulfed cone photoreceptors per RPE cell in *Rev-erbα*$^{+/+}$ and *Rev-erbα*$^{-/-}$ eyes. (C) Mouse primary RPE cells isolated from 8-week-old *Rev-erbα*$^{+/+}$ and *Rev-erbα*$^{-/-}$ mice were challenged with 10 FITC-labeled porcine photoreceptor outer segments (POS) per RPE cell for 2 h at 3 weeks after seeding. POS (green), β-Catenin (magenta), DAPI (blue). Scale bar: 5 μm. (D) Quantification of engulfed POS in *Rev-erbα*$^{+/+}$ and *Rev-erbα*$^{-/-}$ RPE cells after 2 h of treatment. (E) Mouse primary RPE cells isolated from 8-week-old *Rev-erbα*$^{+/+}$ and *Rev-erbα*$^{-/-}$ mice were challenged with 10 microspheres (diameter of 1 μm) per cell for 6 h at 3 weeks after seeding. Microsphere (magenta); β-Catenin (green), DAPI (blue). Scale bar: 5 μm. (F) Quantification of engulfed microspheres/cell by *Rev-erbα*$^{+/+}$ and *Rev-erbα*$^{-/-}$ RPE cells after 6 h of treatment. ***: $P < 0.001$, ****: $P < 0.0001$. Error bars indicate SD. (For interpretation of the references to color in this figure legend, the reader is referred to the Web version of this article.)

cells showed significantly fewer ingested microspheres than the *Rev-erbα*$^{+/+}$ cells, which indicates dampened target recognition and engulfment in *Rev-erbα*$^{-/-}$ RPE cells. We also tested the phagocytic activity in another *in vitro* model, a human RPE cell line ARPE-19, with or without *shRev-erbα* expression which led to successful *Rev-erbα* knockdown (Figs. S4A and B). Consistent with the findings from primary mouse RPE cells, ARPE-19 cells with *Rev-erbα* knockdown exhibited significantly reduced fluorescence intensity upon being fed the fluorescence-labeled microspheres (Figs. S4B and C). In addition, expression of phagocytic engulfment genes (*Cd36* and *MerTK*) was decreased in *Rev-erbα*$^{-/-}$ RPE compared with *Rev-erbα*$^{+/+}$ RPE (Fig. S4D). Altogether, these results suggest that REV-ERBα deficiency significantly dampens phagocytic activity in RPE cells, which may underlie the formation of subretinal deposits and other aging-induced ocular pathologies in *Rev-erbα*$^{-/-}$ eyes.

2.5. *Rev-erbα*$^{-/-}$ eyes have increased levels of oxidative stress during aging

Accumulation of oxidative damage in RPE and photoreceptors has been associated with onset of dry AMD [10]. Previous studies found that REV-ERBα stabilization protects against oxidative stress damage in the lung [47,48] and the liver [49]. To investigate the RPE accumulation of reactive oxygen species (ROS) during aging, general ROS production was measured using 2',7'-dichlorodihydrofluorescein diacetate (DCFDA), a fluorescent marker indicative of hydroxyl, peroxyl and other ROS activity inside the cells, in isolated RPE at 3, 6, and 12 months old. *Rev-erbα*$^{-/-}$ RPEs showed significantly elevated ROS production at both 6 and 12 months old (Fig. 4A). Next, an oxidative stress biomarker 8-hydroxy-2-deoxyguanosine (8-OHdG), indicative of nuclear oxidative DNA damage, was evaluated in *Rev-erbα*$^{+/+}$ and *Rev-erbα*$^{-/-}$ retina sections. Consistent with the H2DCF-DA results (Fig. 4A), *Rev-erbα*$^{-/-}$ RPE demonstrated much stronger 8-OHdG staining in the nucleus (colocalized with DAPI) than *Rev-erbα*$^{+/+}$ RPE at 12 months old, indicating significantly higher nuclear oxidative DNA damage (Fig. 4B). These results suggest that REV-ERBα deficiency leads to increased oxidative stress in aging mouse RPE.

2.6. *Rev-erbα*$^{-/-}$ eyes are more sensitive to oxidative stress-induced RPE and retinal damage

To evaluate whether REV-ERBα deficiency affects RPE health under oxidative stress, an acute model of sodium iodate ($NaIO_3$)-induced RPE and photoreceptor damage was used in mice. Intravenous injection of

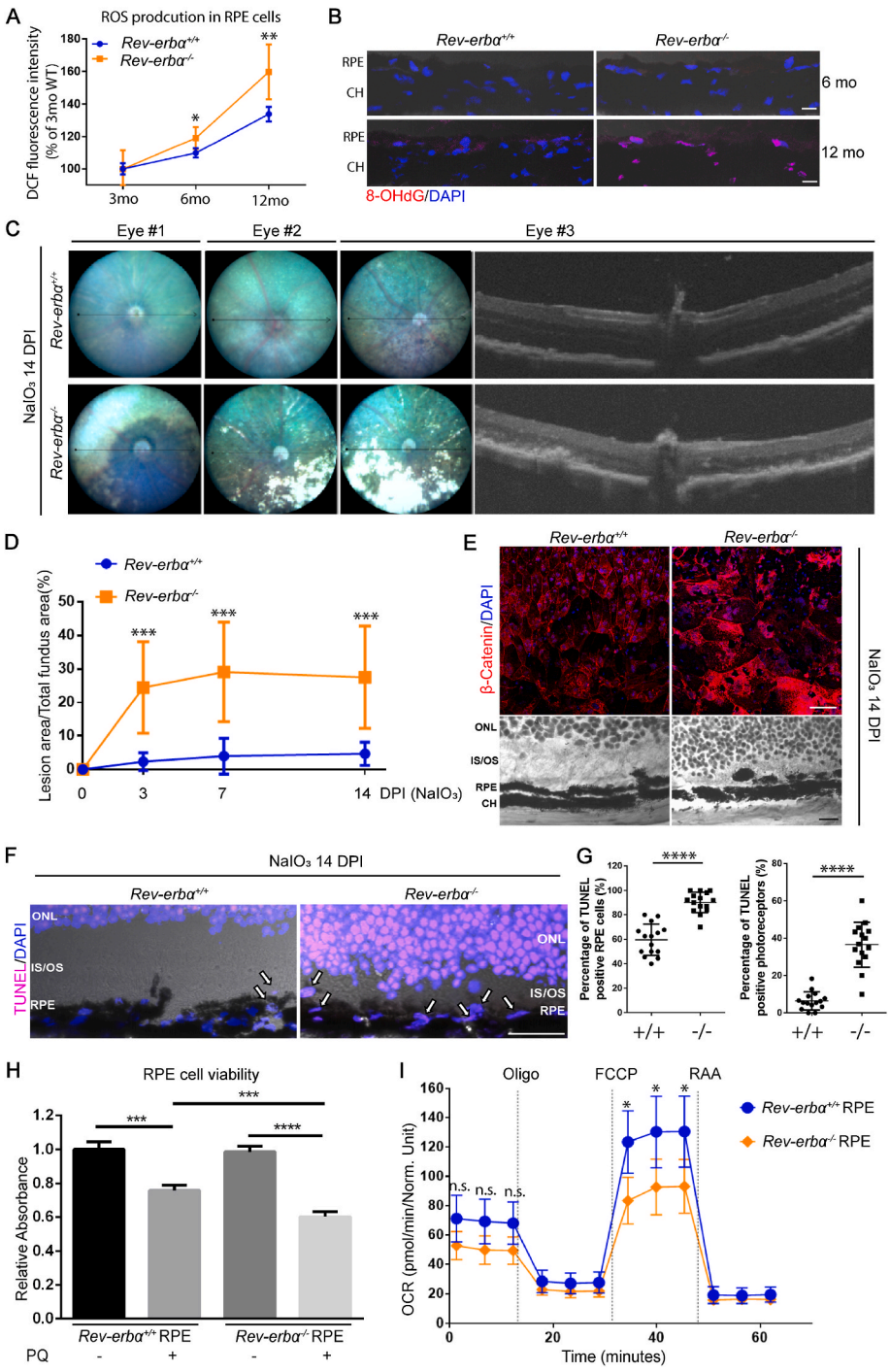

Fig. 4. *Rev-erbα*$^{-/-}$ eyes are more sensitive to chemical-induced oxidative stress injury. (A) Reactive oxygen species (ROS) production was assessed in 3-, 6-, and 12-month-old *Rev-erbα*$^{+/+}$ and *Rev-erbα*$^{-/-}$ RPE cells by using a quantitative cellular ROS assay kit measuring 2',7' –dichlorofluorescin diacetate (DCFDA), a fluorogenic dye indicative of hydroxyl, peroxyl and other ROS activity inside the cells. (B) Representative images of immunostaining of 8-hydroxy-2' -deoxyguanosine (8-OHdG) in 6- and 12-month-old *Rev-erbα*$^{+/+}$ and *Rev-erbα*$^{-/-}$ retinas. Scale bar: 10 μm. (C) Three representative fundus images of *Rev-erbα*$^{+/+}$ and *Rev-erbα*$^{-/-}$ mice and associated OCT images at 14 days post-$NaIO_3$ injection (20 mg/kg body weight, a low dose to evaluate mouse sensitivity to RPE damage). (D) Quantification of RPE atrophy (loss of pigment) in fundus images at 3, 7, and 14 days post-$NaIO_3$ injection. n = 7–8 mice/group. (E) RPE/choroid flat mounts from *Rev-erbα*$^{+/+}$ and *Rev-erbα*$^{-/-}$ mice were stained with β-Catenin (red) and DAPI (blue) at 14 days post-$NaIO_3$ injection (upper panel). Severe RPE loss was observed at peripheral regions of *Rev-erbα*$^{-/-}$ eyes in the RPE/choroid flat mounts, as well as hematoxylin and eosin (H&E) staining of eye cross-sections (lower panel). H&E staining also shows focal loss of outer segments and a discontinued RPE layer in *Rev-erbα*$^{-/-}$ retinas at 14 days post-$NaIO_3$ injection. Scale bar: flat mounts, 50 μm; H&E staining, 10 μm. (F) Representative images of TUNEL staining (magenta) in *Rev-erbα*$^{+/+}$ and *Rev-erbα*$^{-/-}$ eye cross-sections (peripheral regions) co-stained with DAPI (blue) at 14 days post-$NaIO_3$ injection. Arrows indicate TUNEL positive RPE cells. Scale bar: 10 μm. (G) Quantification of the TUNEL positive RPE cells and photoreceptors. n = 15 images/genotype. (H) Primary RPE cells isolated from 8-week-old *Rev-erbα*$^{-/-}$ mice showed decreased cell viability after paraquat (PQ, 0.5 mM, 4 h)-induced oxidative damage compared to *Rev-erbα*$^{+/+}$ RPE cells. n = 6/group. (I) Oxygen consumption rate (OCR) of *Rev-erbα*$^{+/+}$ and *Rev-erbα*$^{-/-}$ primary RPE cells were analyzed after PQ treatment (0.5 mM, 2 h) using Seahorse XFe96 extracellular flux analyzer. *Rev-erbα*$^{-/-}$ RPE cells showed significantly decreased maximal respiratory capacity under oxidative stress compared with *Rev-erbα*$^{+/+}$ RPE cells. *: $P < 0.05$; **: $P < 0.01$; ***: $P < 0.001$; ****: $P < 0.0001$. Error bars indicate SD. (For interpretation of the references to color in this figure legend, the reader is referred to the Web version of this article.)

$NaIO_3$ in mice results in primarily RPE death followed by secondary death of the overlying photoreceptors, similar to what is observed in advanced atrophic AMD [50]. Here $NaIO_3$ was administered to 8-week-old *Rev-erbα*$^{+/+}$ and *Rev-erbα*$^{-/-}$ mice intravenously and the development of RPE and retinal lesions was assessed through fundus and OCT imaging at 3, 7 and 14 days post-injection (Figs. 4C and S5). Significantly worse RPE and retinal damage was observed in *Rev-erbα*$^{-/-}$ eyes, with ~5-fold greater lesion area than *Rev-erbα*$^{+/+}$ eyes, starting from 3 days after $NaIO_3$ administration, and persisting through day 14 (Fig. 4D). Worsened RPE integrity was further confirmed in $NaIO_3$-injected *Rev-erbα*$^{-/-}$ versus *Rev-erbα*$^{+/+}$ eyes with immunostaining of β-catenin in the RPE/choroid flat mounts and H&E staining of cross sections (Fig. 4E). In addition, there was substantially greater RPE cell death (~50% of increase) in *Rev-erbα*$^{-/-}$ than *Rev-erbα*$^{+/+}$ eyes in cross sections measured with terminal deoxynucleotidyl transferase dUTP nick end labeling (TUNEL) staining indicative of both apoptotic and necrotic cells (Fig. 4F and G). These observations suggest that loss of REV-ERBα leads to increased susceptibility of oxidative stress-induced RPE and retinal damage in mice.

Next, the effects of REV-ERBα on RPE oxidative stress was assessed in primary mouse RPE cells *in vitro*. Primary *Rev-erbα*$^{-/-}$ RPE cells have significantly lower cell viability compared to *Rev-erbα*$^{+/+}$ cells, after treatment with paraquat (PQ), a pesticide capable of inducing oxidative stress and subsequent cell death [51] (Fig. 4H). Moreover, oxygen consumption rate in PQ-treated *Rev-erbα*$^{-/-}$ RPE cells showed decreased maximal respiration capacity compared with *Rev-erbα*$^{+/+}$ RPE measured

by Seahorse cell metabolic analysis, without significant change in basal respiration, indicating impaired RPE mitochondrial function upon REV-ERBα deficiency (Fig. 4I). Together, these results show that REV-ERBα-deficient RPE cells are more vulnerable to oxidative stress damage both *in vivo* and *in vitro*.

2.7. REV-ERBα agonist protects RPE from chemical-induced oxidative damage

Since REV-ERBα regulates oxidative stress production in RPE and REV-ERBα deficiency exacerbates RPE oxidative damage, we next assessed if activation of REV-ERBα may protect RPE from oxidative damage. The physiological ligand for the orphan receptor REV-ERBα was first identified as heme in 2007 [35]. Besides heme, REV-ERBα can also be activated by novel synthetic agonists, e.g., SR9009 and SR9011, both *in vitro* and *in vivo* [29,34], which are dual REV-ERBα/β agonists. To activate REV-ERBα in the RPE, SR9009 (100 mg/kg, i.p., b.i.d) was administered to 8-week-old C57BL/6J mice starting from 2 days prior to $NaIO_3$ injection (40 mg/kg body weight), until 7 days post-$NaIO_3$ injection. Activation of REV-ERBα in RPE by SR9009 treatment was confirmed by suppression of known REV-ERBα target genes including *Bmal1* and *Clock* (as common readout of REV-ERBα activation) in isolated RPE samples (Fig. S6B), even though $NaIO_3$ treatment may induce partial downregulation of mRNA expression of *Nr1d1*(REV-ERBα) in WT mice (Fig. S6A). Fundus imaging from SR9009-treated group showed remarkably smaller lesion areas (~40% of reduction) compared with vehicle control group at 7 days post-$NaIO_3$ injection (Fig. 5A). The SR9009-treated group also exhibited ~50% of reduction in RPE cell death compared with the control group in eye cross-sections stained with TUNEL apoptotic staining (Fig. 5B). These data suggest that activation of REV-ERBα protects RPE against $NaIO_3$-induced oxidative damage in mice.

We next sought to determine if REV-ERBα activation directly promotes RPE cell health and survival *in vitro*. Primary RPE cells isolated from C57BL/6J mice were treated with paraquat (PQ) (0.5 mM, 4 h) to induce oxidative stress, followed by either SR9009 or vehicle treatment for 24 h. SR9009-treated RPE cells demonstrated increased oxygen consumption rate in both basal and maximal respiration, indicating that SR9009 may help restore RPE mitochondrial function and cellular health after oxidative damage (Fig. 5C). Additionally, REV-ERBα agonists SR9009 and SR9011 both promoted ARPE-19 cell viability after PQ treatment (Fig. S7A), suggesting their potent cytoprotective effects *in vitro*. In addition, ARPE-19 cells treated with SR9009 exhibited visibly improved mitochondrial morphology (by mitoTracker staining) after PQ-induced oxidative damage (Fig. S7B), and both SR9009 and SR9011 enhanced ARPE-19 cell phagocytic activity (Fig. S7C), indicating that the REV-ERBα activation improves RPE mitochondrial function and phagocytosis *in vitro*. Together, these data suggest that the activation of REV-ERBα markedly protects RPE from oxidative stress-induced cell death, mitochondrial damage and cellular malfunction.

As previous literature has shown that SR9009 is a dual agonist of both REV-ERBα and REV-ERBβ [34], we further examined the specificity of SR9009 on REV-ERBα in mouse RPE. First, mRNA levels of both *Nr1d1* (REV-ERBα) and *Nr1d2* (REV-ERBβ) were assayed from WT mouse RPE. We found *Nr1d1* expression is ~5 fold higher than *Nr1d2* in mouse RPE cells (Fig. S8A). Second, MTT assay showed that the REV-ERB agonist SR9009 only preserved viability of *Rev-erbα*$^{+/+}$ primary RPE cells after PQ treatment, yet failed to protect *Rev-erbα*$^{-/-}$ primary RPE cells from

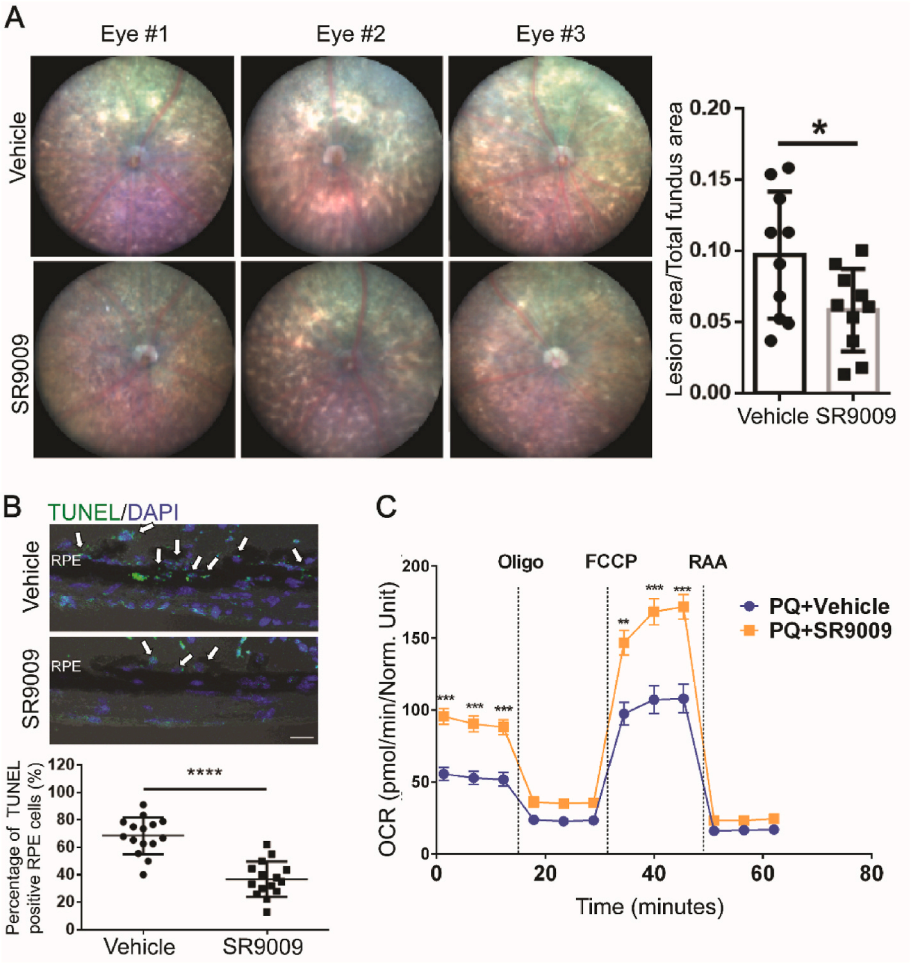

Fig. 5. REV-ERBα agonist protects against chemical ($NaIO_3$)-induced RPE damage. (A) Representative fundus images of vehicle and SR9009 (100 mg/kg body weight)-treated WT mice at 7 days post-$NaIO_3$ injection (40 mg/kg body weight, a medium dose to evaluate drug protection against RPE damage), with quantification of lesion area per fundus image for each group. Sample size: $NaIO_3$ injection, n = 5 mice/group; fundus quantification, n = 10 images (eyes)/group. (B) TUNEL staining (green) and quantification of TUNEL positive RPE cells (arrows) in the cross-sections (peripheral regions) of vehicle- and SR9009-treated retinas at 7 days post-$NaIO_3$ injection. Blue: DAPI staining. Scale bar: 10 μm. n = 15 images/group. (C) WT primary RPE cells were first challenged by PQ (0.5 mM, 4 h), followed by vehicle or SR9009 (1 μm, 24 h) treatment. Oxygen consumption rate (OCR) was then analyzed using Seahorse XFe96 extracellular flux analyzer. SR9009-treated RPE cells showed significantly improved basal and maximal respiratory capacity under oxidative stress compared to vehicle-treated cells. *: $P < 0.05$, **: $P < 0.01$, ***: $P < 0.001$, ****: $P < 0.0001$. Error bars indicate SD. (For interpretation of the references to color in this figure legend, the reader is referred to the Web version of this article.)

oxidative damage (Fig. S8B). Third, we performed $NaIO_3$ treatment (40 mg/kg) in 6 months old *Rev-erbα*$^{-/-}$ mice injected with either vehicle or SR9009 (100 mg/kg b.i.d.). We found that SR9009 also failed to show protective function and reduce lesion area 7 days after $NaIO_3$ treatment in *Rev-erbα*$^{-/-}$ eyes (Fig. S8C). These findings suggest that the RPE protective effects of SR9009 depends on the presence of REV-ERBα in mouse RPE cells, establishing the specificity of SR9009 on REV-ERBα in RPE protection and eliminating potential off-target effects through REV-ERBβ.

2.8. REV-ERBα regulates NRF2 transcription and its downstream target antioxidant genes in RPE

As a transcriptional regulator, REV-ERBα plays an integral role in regulating the expression of target genes involved in circadian rhythm, lipid biogenesis, and mitochondrial biogenesis [25,28,37]. Our findings so far suggest that REV-ERBα regulates RPE oxidation status. Healthy RPE maintains cellular redox homeostasis through an endogenous antioxidant defense system to counter oxidative stress and cellular damage, with NRF2 (encoded by *Nfe2l2*) as a key cytoprotective factor. Elimination of ROS in RPE is carried out primarily by a NRF2-dependent antioxidant self-defense mechanism, including SOD (superoxide dismutase), catalase, and peroxidase, in addition to free radical scavengers [52]. In order to examine if REV-ERBα transcriptionally regulates RPE antioxidant self-defense system, mRNA expression of several anti-oxidative enzymes (*Sod1*, *Sod2*, and *catalase*) and their master regulator NRF2 (*Nfe2l2*) were assessed, all of which are downregulated in *Rev-erbα*$^{-/-}$ RPE (Fig. 6A), in addition to downregulation of *Gpx1/4* (glutathione peroxidase 1 and 4) and *Homx2* (heme oxygenase 2) (Fig. S9A), indicating potential positive regulation of these genes by REV-ERBα**.** Protein levels of nuclear NRF2 (110 kDa, with ubiquitination), SOD1 and catalase were consistently lower in *Rev-erbα*$^{-/-}$ RPE compared to those of *Rev-erbα*$^{+/+}$ (Fig. 6B).

As a transcription factor, NRF2 is a key upstream regulator of antioxidative enzymes including SOD1, SOD2 and catalase [13]. NRF2 deficiency has been highly correlated with age-related retinal degeneration and RPE damage in mice [17]. We thus investigated if REV-ERBα activates NRF2 (*Nfe2l2*) and thereby regulates its downstream target genes including *Sod1/2, Cat* (catalase), *Gpx1/4*, and *Hmox2*. Protein levels of NRF2, SOD1, SOD2 and catalase were measured in RPE isolated from SR9009-treated mice in the $NaIO_3$ damage model. Notably, SR9009 administration significantly increased the protein levels of NRF2, SOD1 and catalase in RPE *in vivo* (Fig. 6C). In ARPE-19 cells, both SR9009 and SR9011 substantially increased the mRNA expression of *NFE2L2*, *SOD1/2*, *CAT*, and other NRF2 target genes under oxidative stress in a dose responsive manner (Fig. S9B&C). Induction of NRF2 and SOD1 protein levels by REV-ERBα agonists was also confirmed by Western blotting (Fig. S9D). These results suggest that REV-ERBα induces NRF2 (*Nfe2l2*), SOD1 (*Sod1*) and catalase (*Cat*) expression in RPE cells *in vivo* and *in vitro* at both mRNA and protein levels.

To explore whether REV-ERBα may activate these antioxidant enzymes through NRF2, we performed a chromatin immunoprecipitation (ChIP) assay with REV-ERBα antibody followed by qPCR in ARPE-19 cells to determine if REV-ERBα directly binds to the regulatory region of NRF2 (*NFE2L2*). REV-ERBα usually binds to the regulatory DNA regions of its target genes through a conserved RORE/RevRE motif with a consensus core sequence of AGGTCA [53–55]. Sequence analysis identified three RORE motifs from 2,000 bps upstream of the *NFE2L2* transcription start site (TSS) (−2000) to 500 bps in its 5′-untranslated region (UTR) (+500) (Fig. 6D). Three pairs of primers were designed to flank each RORE/RevRE motif. The strongest enrichment was found in RORE/RevRE #1 site (+295 ~ +302 bps of *NFE2L2* gene) in DNA fragments precipitated by REV-ERBα monoclonal antibody, at a level comparable with known REV-ERBα target gene *BMAL1* as a positive control (Fig. 6E). Enrichment of RORE/RevRE #1 binding site was further enhanced by treatment with REV-ERBα agonist SR9009 (vs. control), and abolished in cells treated with shRNA targeting REV-ERBα (vs. control shRNA) (Fig. 6E).

REV-ERBα is a known transcriptional repressor [55,56], but in some cases has also been reported as a activator [31,54]. The direct transcription repressor role of REV-ERBα has been extensively studied in various organs, particularly for circadian regulatory genes [23], yet for other genes, especially metabolic genes, it has been suggested that indirect transcriptional regulation by REV-ERBα is also likely and through other transcription mediators [31,57]. Two transcriptional co-regulatory proteins, HDAC3 and NCOR1, are co-factors of REV-ERBα that can be recruited by REV-ERBα onto the RORE/RevRE binding sites [58]. However, a recent ChIP-Seq assay has shown that a large portion of REV-ERBα binding sites does not overlap with either HDAC3 or NCOR1 in the genome [59], indicating that REV-ERBα may interact distinctly with DNA fragments in a HDAC3/NCOR1-independent manner. We therefore conducted a ChIP assay to immunoprecipitate HDAC3 and NCOR1, and probe for NRF2 RORE/RevRE #1 site. Our ChIP assay did not identify an interaction of either HDAC3 or NCOR1 with NRF2 RORE/RevRE #1 (Fig. 6F), although both HDAC3 and NCOR1 interact with RORE/RevRE motif in *BMAL1* DNA sequence as expected (Fig. 6F). These results suggest that REV-ERBα binds a single RORE/RevRE fragment located at the 5′-UTR of *NFE2L2* gene, and that this monomeric binding is independent from the HDAC3/NCOR1 interaction, potentially similar to what was reported for REV-ERBα regulation of metabolic genes or reflecting that more than one closely located RORE/RevRE sites are required for cofactor recruitment and binding [30,59].

We next conducted luciferase reporter assays to determine if the interaction between REV-ERBα and the *NFE2L2* RORE/RevRE #1 binding site contributes to *NFE2L2* transcription. The native *NFE2L2* 5′-UTR from +164 to +466, which includes the RORE/RevRE #1 element; and a fragment of −898∼-716 of *NFE2L2* promoter, which included the RORE/RevRE #3 element (as a negative control), were cloned into a pGL3 vector, then expressed in ARPE-19 cells. ARPE-19 cells expressing *NFE2L2* RORE/RevRE #1 site showed substantially higher (∼5-fold) luciferase activity, indicative of *NFE2L2* promoter activity, compared with blank vector control and #3 site. Moreover, we further treated the ARPE-19 cells with either the REV-ERBα agonist SR9009, or p3Flag-REV-ERBα plasmid overexpressing REV-ERBα, with confirmed overexpression of Flag-tagged REV-ERBα (Fig. 6G). Both treatments further enhanced luciferase reading of *NFE2L2* promoter activity by over 3-fold in the *NFE2L2* RORE/RevRE #1 site-expressing cells in comparison to the vehicle control treatment, but not in blank vector control and RORE/RevRE #3 site-expressing cells (Fig. 6H). Together, these findings suggest that REV-ERBα induces the transcription of NRF2 (*NFE2L2)* and thereby increases expression of its downstream target genes such as SOD1 and catalase to counter oxidative damage in RPE.

2.9. RPE specific knockout of REV-ERBα in mice results in fundus and RPE pathologies similar to Rev-erbα$^{-/-}$ mice

To investigate if REV-ERBα deficiency in RPE cells alone is sufficient to cause age-related oxidative damage in mouse eyes and to delineate any potential influence of systemic factors, mice with RPE specific knockout of REV-ERBα were generated by crossing *Rev-erbα* flox mice (*Rev-erbα*$^{fl/fl}$) with mice expressing Cre recombinase under the control of the human bestrophin 1 promoter (*BEST1-cre*), which is primarily RPE specific [60]. Knockout efficiency of REV-ERBα was confirmed at both mRNA and protein levels with up to 80% of knockdown in *BEST1-cre: Rev-erbα*$^{fl/fl}$ RPE (Fig. 7A, B, and H). Immunostaining of REV-ERBα also demonstrated absence of REV-ERBα in *BEST1-cre: Rev-erbα*$^{fl/fl}$ RPE flat mounts (Fig. 7C), and the specificity of REV-ERBα knockdown in RPE cells but not other retinal cell types in the eye cross sections (Fig. 7D). Fundus imaging of *BEST1-cre: Rev-erbα*$^{fl/fl}$ mice showed a significantly greater number of whitish yellow lesions at both 6 and 9 months old, compared to both *Rev-erbα*$^{fl/fl}$ and *BEST1-cre* control mice (Fig. 7E and

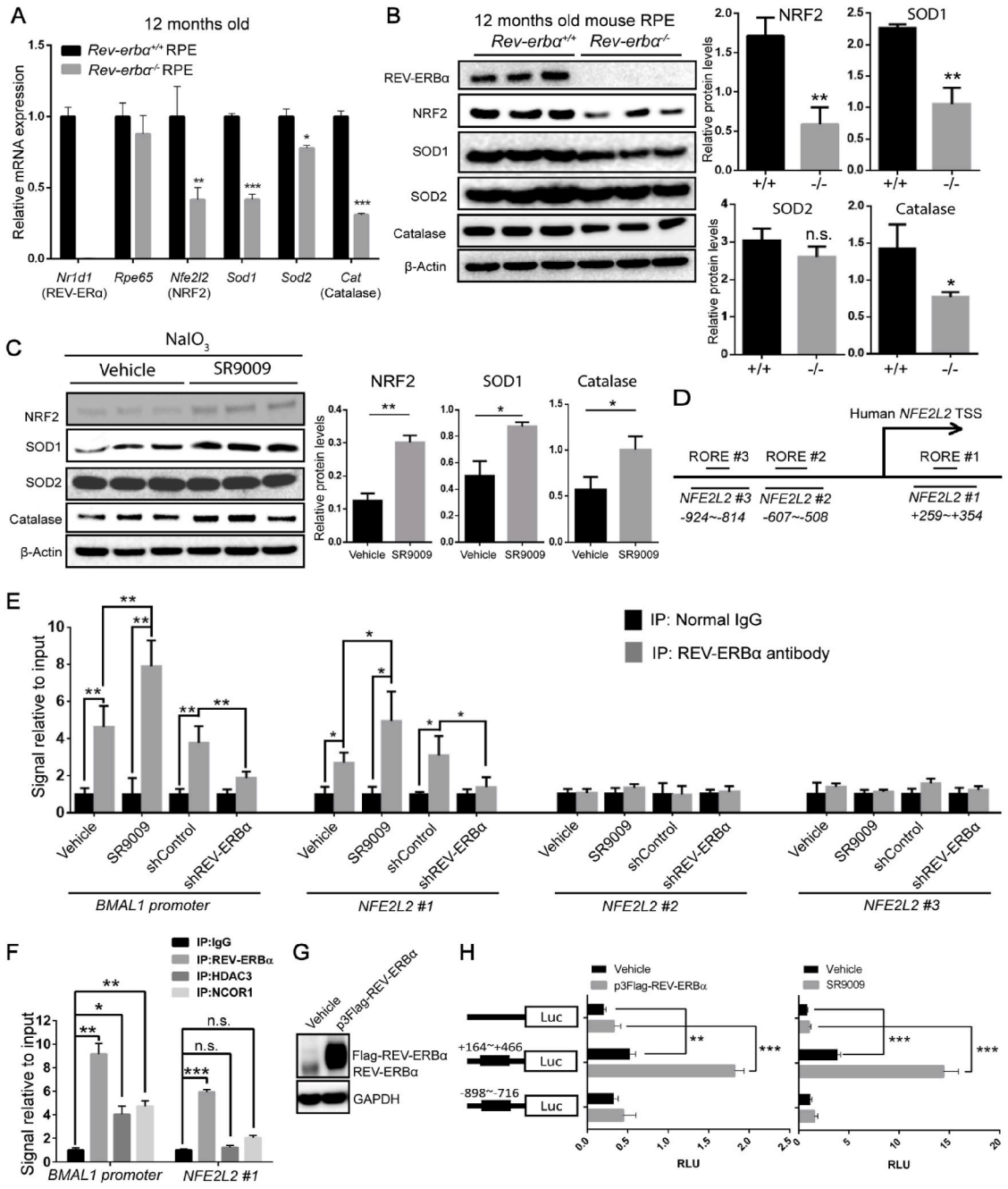

Fig. 6. REV-ERBα regulates NRF2(*Nfe2l2*) transcription and the expression of its downstream target antioxidant genes in RPE cells. (A) mRNA expression of NRF2 (*Nfe2l2*) and its downstream target antioxidant genes (*Sod1, Sod2, Cat)* in the RPEs of 12-month-old *Rev-erbα*$^{+/+}$ and *Rev-erbα*$^{-/-}$ mice. Real-time q-PCR results were normalized to *18S* and then normalized again to the expression levels in *Rev-erbα*$^{+/+}$ RPE cells. n = 6/group. (B) Western blot and quantification of NRF2, SOD1, SOD2, and catalase protein levels in 12-month-old *Rev-erbα*$^{+/+}$ and *Rev-erbα*$^{-/-}$ RPEs, with a confirmation of REV-ERBα knockout. Protein sizes: nuclear NRF2 (110 kDa), SOD1 (20 kDa), SOD2 (20 kDa), catalase (60 kDa). n = 3 eyes/group. (C) Protein levels of NRF2, SOD1, SOD2 and catalase were assayed and quantified in the primary RPE cells from vehicle- and SR9009-treated mice after $NaIO_3$ injection by Western blotting. n = 3 eyes/group. (D) A schematic diagram shows RORE/RevRE elements across the human *NFE2L2* (NRF2) upstream regulatory region. The thick truncated lines mark the regions covered by 3 primer sets of interest (*NFE2L2 #1 + 259~+354, NFE2L2 #2 –607~-508, NFE2L2 #3 –924~-814*). TSS: Transcription start site. (E) Chromatin-immunoprecipitation (ChIP) assays for binding of REV-ERBα with the regulatory region upstream of the *NFE2L2* gene. The ChIP assay was conducted to analyze the local enrichment of REV-ERBα-associated ROREs across the upstream regulatory region and part of 5′UTR of the *NFE2L2* gene in ARPE19 cells under four conditions: vehicle vs. SR9009 treatment and shControl vs. sh*REV-ERBα*. In addition to probing for *NFE2L2 #1, NFE2L2 #2, NFE2L2 #3*, a pair of primers covering the RORE of the *BMAL1* promoter was probed as a positive control. The relative fold enrichment was quantified by normalization to input, and then normalized against the levels in normal rabbit IgG pulled down groups. n = 6/group. (F) ChIP assay was conducted to analyze the local enrichment of DNA fragments containing the *NFE2L2 #1* region in ARPE-19 cells with REV-ERBα, HDAC3 and NCOR1 antibodies pull down. The relative fold enrichment was quantified by normalization to input, and then against the levels in IgG group. n = 6/group. (G) Western Blot analysis of ARPE-19 cells transfected with either vehicle or p3Flag-REV-ERBα confirmed over-expression of flag-tagged REV-ERBα (Flag-REV-ERBα), with slightly higher MW than native REV-ERBα. (H) Luciferase assay was conducted in ARPE19 cells transfected with pGL3 (empty vector), pGL3-NFE2L2 #1 (+164~+466), and pGL3-NFE2L2 #3 (−898~-716) with vehicle vs. p3Flag-REV-ERBα, or vehicle VS. SR9009. Relative luminescence units (RLU) were quantified after normalizing to *Renilla* luciferase. n.s.: not significant, *: $P < 0.05$, **: $P < 0.01$, ***: $P < 0.001$****: $P < 0.0001$. Error bars indicate SD.

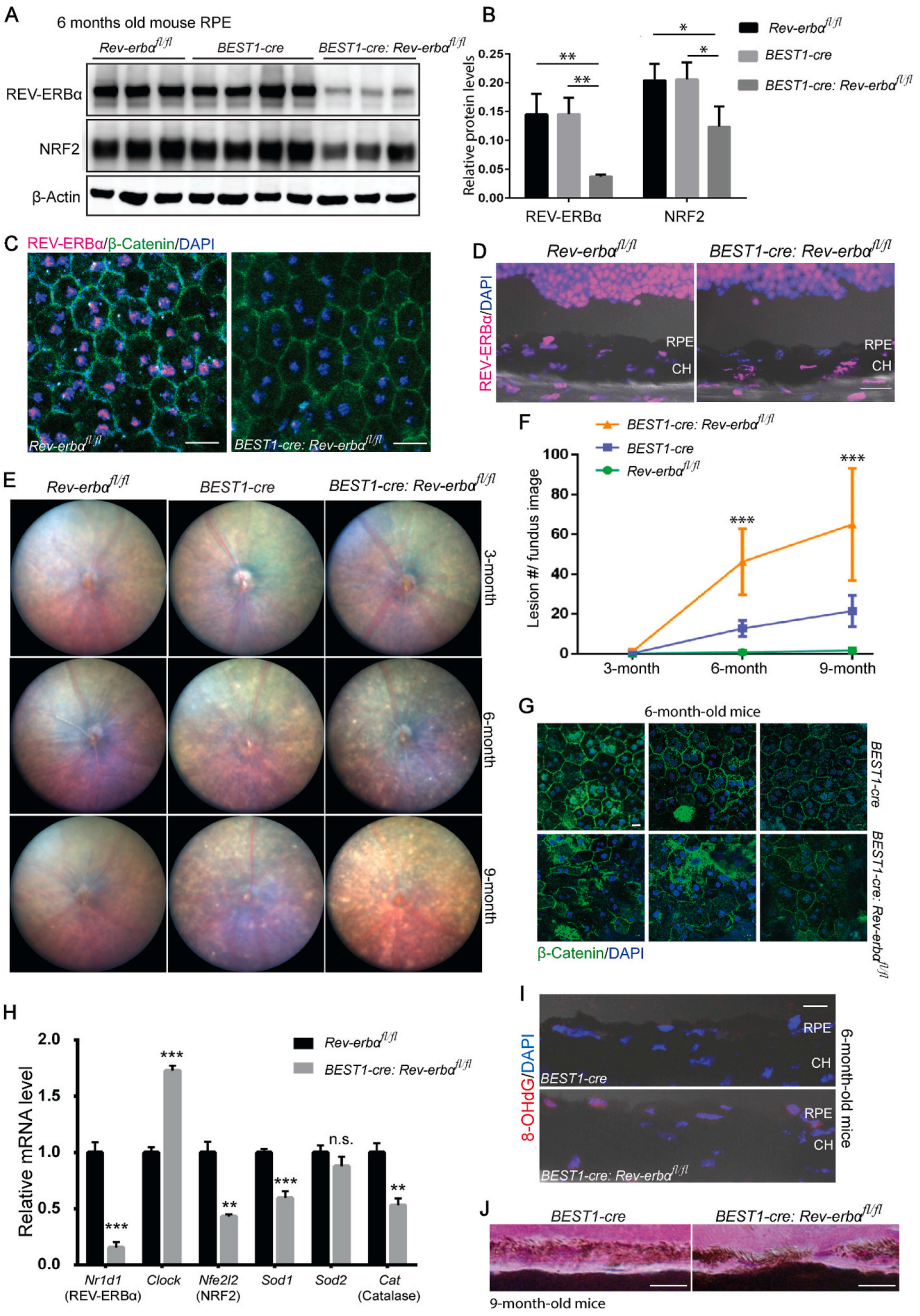

Fig. 7. RPE-specific knockout of REV-ERBα in mice shows similar ocular pathologies as *Rev-erbα*$^{-/-}$ mice. (A–B) Protein levels of REV-ERBα and NRF2 were assayed (A) and quantified (B) in *Rev-erbα*$^{fl/fl}$, *BEST1-Cre,* and *BEST1-cre: Rev-erbα*$^{fl/fl}$ RPEs by Western blotting. The *BEST1-cre: Rev-erbα*$^{fl/fl}$ RPE showed ~75% efficiency of REV-ERBα knockout at protein levels, and NRF2 protein levels were down-regulated by ~40% in *BEST1-cre: Rev-erbα*$^{fl/fl}$ RPE. n = 3–4 mice/group. (C–D) Immunohistochemistry confirmed absence of REV-ERBα (magenta) in RPE/choroid flat mounts (C) counterstained with β-catenin (green) and DAPI (blue) and cross-sections (D) in 3-month-old *BEST1-cre: Rev-erbα*$^{fl/fl}$ vs. *Rev-erbα*$^{fl/fl}$ mice. Scale bars, C: 20 μm; D: 20 μm. (E) *Rev-erbα*$^{fl/fl}$, *BEST1-Cre,* and *BEST1-cre: Rev-erbα*$^{fl/fl}$ mice were examined by fundus imaging at 3, 6, and 9 months old. *BEST1-cre: Rev-erbα*$^{fl/fl}$ retinas showed whitish lesions starting from 6 months old. (F) Quantification of lesion numbers in fundus images of *Rev-erbα*$^{fl/fl}$, *BEST1-Cre,* and *BEST1-cre: Rev-erbα*$^{fl/fl}$ eyes shows significant difference in lesion count in *BEST1-cre: Rev-erbα*$^{fl/fl}$ eyes vs. both *BEST1-Cre, and Rev-erbα*$^{fl/fl}$ control groups. n = 10–16 eyes/group, mixed genders. (G) Immunohistochemistry of β-catenin (green) and DAPI (blue) in *BEST1-cre: Rev-erbα*$^{fl/fl}$ RPE/choroid flat mounts showed more severe patchy, distorted RPE cells than *BEST1-cre* mice. Scale bar, 10 μm. (H) mRNA expression of *Nr1d1* (REV-ERBα), *Clock* (positive control), *Nfe2l2* (NRF2), *Sod1, Sod2 and catalase* was examined in the RPE of 6-month-old *Rev-erbα*$^{fl/fl}$ and *BEST1-cre: Rev-erbα*$^{fl/fl}$ mice. qPCR results were normalized to *18S* and then normalized again to the expression levels in *Rev-erbα*$^{fl/fl}$ RPE cells. n = 6/group. (I) Representative images of immunostaining of 8-OHdG in 6-month-old *BEST1-cre and BEST1-cre:Rev-erbα*$^{fl/fl}$ retinas. Scale bar, 10 μm. (J) Representative images of H&E staining showed discontinued RPE layer in 9-month-old *BEST1-cre: Rev-erbα*$^{fl/fl}$ vs. *BEST1-cre* eye cross-sections. Scale bar, 10 μm **: $P < 0.01$, ***: $P < 0.001$****: $P < 0.0001$. Error bars indicate SD. (For interpretation of the references to color in this figure legend, the reader is referred to the Web version of this article.)

F), although *BEST1-cre* mice also exhibited modest numbers of lesions at 6 and 9 months old due to reported adverse effects of the Cre recombinase presence in RPE cells [61]. In addition, compared with *BEST1-cre* control mice, *BEST1-cre:Rev-erbα*$^{fl/fl}$ mice displayed much more patchy and distorted RPE cells in RPE/choroid flat mounts by immunostaining of β-Catenin and DAPI (Fig. 7G), and more discontinuous RPE in eye cross-sections (Fig. 7J), indicating more severe RPE degeneration. Together these findings suggest that RPE specific knockout of REV-ERBα leads to fundus lesions and RPE degeneration similar to what is observed in *Rev-erbα*$^{-/-}$ mice, demonstrating an RPE cell-autonomous role of REV-ERBα in regulating RPE function and health.

Next, we examined if RPE-specific knockout of REV-ERBα also transcriptionally regulates NRF2 (*Nfe2l2)* and its downstream antioxidant genes, similar to the findings in REV-ERBα systemic knockout mice (Fig. 6). Protein levels of NRF2 were substantially decreased in *BEST1-cre:Rev-erbα*$^{fl/fl}$ RPE by ~40% vs. both flox and cre controls: *Rev-erbα*$^{fl/fl}$ and *BEST1-cre* RPE by Western blotting (Fig. 7A and B). In addition, RPE expression of *Nfe2l2*, *Sod1*, *Sod2* and *Cat* was examined in *Rev-erbα*$^{fl/fl}$, and *BEST1-cre:Rev-erbα*$^{fl/fl}$ RPE at 6 months old (using known REV-ERBα target gene *Clock* as a positive control). Similar to REV-ERBα systemic knockout mice, *BEST1-cre: Rev-erbα*$^{fl/fl}$ RPE showed substantially decreased mRNA levels of *Nfe2l2*, *Sod1* and *Cat* compared to *Rev-erbα*$^{fl/fl}$ RPE (Fig. 7H). To examine if REV-ERBα deficiency specifically in RPE alters RPE cell oxidative status, 8-OHdG staining was performed. *BEST1-cre: Rev-erbα*$^{fl/fl}$ mice with REV-ERBα knockout in RPE cells had strong positive staining of 8-OhDG at 6 months old (Fig. 7I), compared with absence of 8-OHdG staining in *BEST1-cre* mice, even though *BEST1-cre* mice exhibited modest fundus lesions and RPE damage (Fig. 7F and G). Together, these findings suggest that the RPE-specific knockout of REV-ERBα sufficiently reduces

NRF2 (*Nfe2l2)* transcription within RPE and may thus lead to weakened antioxidant self-defense and increased oxidative stress, thereby damage in RPE cells.

3. Discussion

Our results reveal a novel role of REV-ERBα in protecting RPE health and function from oxidative damage and aging. We found that: 1) genetic deficiency of REV-ERBα leads to RPE degeneration and atrophy in mice, with sub-retinal accumulation of extracellular proteins and lipids; 2) loss of REV-ERBα impairs RPE phagocytic function in mice; 3) REV-ERBα deficiency exacerbates oxidative damage ($NaIO_3$)-induced RPE and retinal toxicity *in vivo*; 4) pharmacological activation of REV-ERBα protects against chemically induced RPE oxidative damage *in vivo* and *in vitro*; 5) REV-ERBα transcriptionally activates the expression of NRF2, a cytoprotective transcription factor, and its downstream antioxidant enzymatic genes; 6) RPE-specific deletion of REV-ERBα reproduces similar RPE and fundus pathologies as seen in systemic knockout mice. These data demonstrate that REV-ERBα is a critical intrinsic redox-sensitive protector of RPE function and health and acts by enhancing the intracellular antioxidant defense system. Activating REV-ERBα may serve as a new way to counter RPE oxidative damage and preserve the RPE in age-related retinal degeneration (Fig. S10).

Prior studies found that REV-ERBα regulates transcriptional networks critical for photoreceptor development and function [26]. Specifically, it functions as a transcription activator in rod photoreceptors in conjunction with its cofactor NR2E3, a photoreceptor-specific nuclear receptor [39]. Knockdown of REV-ERBα in mouse eyes results in pan-retinal spotting and reduced response to light in scotopic (dark-adapted) and photopic (light-adapted) experiments [26]. However, no gross morphological abnormality was reported in H&E or immunohistochemical stained sections of REV-ERBα-knockdown retinas at young age [26]. This suggest that either partial knockdown was not sufficient to cause detectable retinal pathologies at this age or that any potential knockdown induced RPE damage in the sub-retinal region may not be noticed or detected. Our data here showed that REV-ERBα expression declined with age in RPE cells, which indicated a potential protective role of REV-ERBα in RPE cells. Consequently, we observed pan-retinal fundus lesions in aging mice with both systemic and RPE-specific knockout of REV-ERBα, and the number of lesions increases with age. Moreover, other AMD-like lesions, including sub-retinal drusenoid-like deposits, RPE degeneration and thickened Bruch's membrane were also found in REV-ERBα deficient eyes, suggesting that the potential utility of *Rev-erbα*$^{-/-}$ mice as a new animal model to investigate AMD pathogenesis involving RPE atrophy. Retinal thickness remained comparable between *Rev-erbα*$^{+/+}$ and *Rev-erbα*$^{-/-}$ eyes at 11 months old (Fig. S11), indicating lack of primary retinal degeneration. In addition, both *in vivo* and *in vitro* findings showed dampened RPE phagocytosis in the absence of REV-ERBα, although whether potential changes in apical microvilli in RPE may contribute to impaired phagocytosis is not yet clear. These results together suggest that loss of REV-ERBα negatively impacts RPE health and accelerates RPE aging in mouse eyes.

REV-ERBα is a well-studied regulator of circadian rhythm [23,62], lipid and glucose metabolism [27,63], and adipogenesis [64] in organs such as liver, brain, lung, and muscle. Several studies also suggested that REV-ERBα plays a role in the oxidative stress response. For example, mRNA expression of REV-ERBα was increased in neonatal (but not adult) mouse lungs exposed to short-term hyperoxia [47], suggesting that REV-ERBα expression may respond to acute oxidative stress in the lung. Another study showed that mRNA levels of REV-ERBα in lung were significantly decreased after an 18-day exposure to cigarette smoke in adult mice [65], indicating a diminished expression of REV-ERBα and thus potentially dampened protection by REV-ERBα under chronic oxidative stress. Moreover, neonatal mouse lung fibroblasts transfected with stabilized REV-ERBα showed upregulated mRNA levels of antioxidant genes including *Foxo 1, Sod2, Cat and Hmox1* under normal conditions, and reduced cell death upon administration of high dose H_2O_2 treatment [48]. Here we provided evidence that protein levels of REV-ERBα decline with age and are downregulated upon chemical-induced oxidative damage in adult mice. Furthermore, loss of REV-ERBα significantly reduces the RPE expression of antioxidant genes such as *Nfe2l2* (NRF2), *Sod1* and *Catalase* in mice, and results in remarkably increased vulnerability of the RPE under chemical-induced oxidative damage and during aging. These data indicate that REV-ERBα may function to sense redox homeostasis accumulated oxidative stress in aged RPE, and protect RPE cells against oxidative damage primarily through the transcriptional activation of antioxidant genes. REV-ERBα deficiency or decreased expression during aging may thus lead to weakened antioxidant defense in RPE cells.

Generation of ROS and oxidative damage has long been considered harmful for RPE functions and health in AMD pathogenesis. For instance, oxidative stress inhibits phagocytic function of RPE cells through the downregulation of phagocytosis-related gene expression [66]. Advanced oxidative damage can also promote RPE senescence [67] and necrotic RPE death [68]. Genetically engineered mouse models lacking antioxidant genes have been shown to mimic pathological manifestations in human AMD patients, and are thus often used as disease models. In particular, *Nrf2*$^{-/-}$ mice developed elements of AMD-like pathologies including drusen-like and RPE abnormalities during aging [17]. Similarly, *Sod1*$^{-/-}$ mice exhibit drusen-like deposits, RPE dysfunction and atrophy, as well as choroidal neovascularization and progressive retinal degeneration [69]. Mice with RPE-specific knockout of the *Sod2* gene also have alterations in RPE morphology and function [70]. In this study, we found that the protective role of REV-ERBα in RPE is mediated primarily through promoting antioxidant response via its transcriptional regulation of *Nfe2l2* gene. We demonstrate that REV-ERBα transcriptionally activates *Nfe2l2* in RPE cells and thereby promotes the production of antioxidant enzymes downstream of NRF2, including SOD1 and catalase. Loss of REV-ERBα results in increased ROS accumulation and oxidative damage to the RPE cells in aged mice, which induces RPE pathology including RPE dysfunction in phagocytosis, changes in RPE morphology, as well as RPE atrophy. Elevated oxidative stress in *Rev-erbα*$^{-/-}$ RPE is likely due to down-regulation of NRF2, SOD1 and catalase. In the $NaIO_3$-induced RPE damage model, REV-ERBα deficiency leads to increased sensitivity to $NaIO_3$ damage and elevated RPE death due to oxidative injury. Pharmacological activation of REV-ERBα significantly raised the expression of NRF2, SOD1 and catalase in RPE, and slowed down the progression of $NaIO_3$-induced RPE damage in WT mice, demonstrating the therapeutic potential of REV-ERBα activation.

REV-ERBα was first described as a transcription activator *in vitro* [54]. Yet later work found that REV-ERBα markedly repressed the basal activity of a variety of promoters thus inhibited the expression of its target genes, including circadian rhythm-related factors *BMAL1* [23] and *CLOCK* [38], and metabolism-related genes phosphoenolpyruvate carboxykinase (*PCK*) [71] and glucose-6-phosphatase (*G6P*) [72]. This is primarily explained by the fact that the structure of REV-ERBα lacks the carboxy-terminal AF2 region, and hence it cannot bind co-activators [55]. However, a few other studies have reported that REV-ERBα also induces gene expression, such as C/EBP Homologous Protein (CHOP) in the liver [31], and several phototransduction genes in rod photoreceptors [39], similar to our findings of NRF2 induction. Notably, ChIP-seq assays conducted in mouse brain, liver and epididymal adipose tissue showed that REV-ERBα also regulates gene expression through mechanisms independent of direct DNA binding [73]. In our study, we found that REV-ERBα works as a transcriptional activator of *NFE2L2* and induces *NFE2L2* 5'UTR regulatory activity in a luciferase reporter assay. Moreover, REV-ERBα associates with the *NFE2L2* 5'UTR regulatory region, without its typical co-factor NCOR1 or co-regulator HDAC3. Our findings are consistent with prior ChIP-seq data from mouse liver [74], where three putative REV-ERBα binding sites were identified in regulatory regions of *Nfe2l2*. Together these data suggest that REV-ERBα

activates the mRNA expression of *NFE2L2* in RPE cells, and that this activation may or may not act through direct DNA binding.

REV-ERBα is universally expressed throughout many cell types in the body with low tissue specificity. To pinpoint the cell specific role of REV-ERBα in RPE, we used the RPE-specific deletion of REV-ERBα to rule out systemic and paracrine effects of REV-ERBα knockout in mice. Although the RPE-specific Cre recombinase protein (*BEST1-cre*) presents incomplete recombination efficiency and moderate cytotoxicity in RPE cell [61], we observed significantly elevated oxidative damage and impaired RPE integrity in the eyes with RPE-specific knockout of REV-ERBα. In addition, oxidation-induced DNA damage was only observed in RPEs expressing both *BEST1-cre* and *Rev-erbα flox/flox*, but not in RPEs expressing only *BEST1-cre*. This confirms that it is the loss of REV-ERBα, instead of Cre recombinase expression, that results in oxidative damage in the RPE. Importantly, both mRNA and protein levels of NRF2 were downregulated in mouse RPEs with RPE-specific REV-ERBα deletion, which is consistent with what we found in systemic REV-ERBα knockout mice. Altogether, our data suggest that REV-ERBα deficiency in the RPE is sufficient to dampen NRF2 signaling, thereby promoting ROS accumulation and oxidative damage, and negatively impacting overall RPE health and aging.

Although our study provides new insights on a previously undiscovered role of REV-ERBα in the oxidative stress response in the eye, there are some limitations that still need further investigation. First, further examinations are needed to dissect the detailed molecular mechanisms underlying transcriptional interaction of REV-ERBα with *NFE2L2* DNA to results in its transcriptional activation. REV-ERBα may repress another intermediate transcriptional repressor, for example NFIL3/E4BP4, which is a REV-ERBα target gene [24], or other unknown repressors, to result in transactivation of NRF2 by REV-ERBα. Alternatively, negative DNA response elements were suggested to mediate negative transcriptional regulation by glucocorticoid receptor [75], similar negative elements may exist for REV-ERBα as well to lead to transcriptional activation by a known repressor. Second, NRF2 activity is highly regulated by the KEAP1-NRF2 pathway, which controls the activation and degradation of NRF2 protein [14]. Whether REV-ERBα interacts with the KEAP1 regulation of NRF2 pathway is still unknown and deserves further studies. Moreover, beyond regulation of oxidative stress and antioxidant response, REV-ERBα is involved in many other processes including lipid metabolism and circadian control, dysregulation of these processes may also impact RPE health and AMD, that will await further investigation. Potential compensatory cellular and molecular responses may also occur in the absence of REV-ERBα, that will need to be taken into account in our interpretation of the results. Particularly, specificity of SR ligands on REV-ERB has been controversial regarding its potential REV-ERB-independent off target effects [76], yet our data showed SR9009 lost its protective effects on REV-ERBα deficient mice and RPE cells, strongly suggesting that its protection of RPE is REV-ERBα dependent.

In conclusion, our findings uncover a novel transcriptional control mechanism mediated by REV-ERBα that links the RPE redox environment with age-related RPE dysfunction and degeneration. Loss of REV-ERBα accelerates RPE aging and leads to AMD-like ocular pathologies in mice. Activation of REV-ERBα may counter oxidative damage in RPE via enhancing NRF2-dependent antioxidant defense system. Together this work not only identified the *Rev-erbα*$^{-/-}$ mice as a novel animal model for studying AMD, but also established REV-ERBα as a new potential druggable target for developing future therapeutics in order to preserve RPE health in dry AMD.

4. Materials and methods

4.1. Study design

All animal experiments were approved by the Institutional Animal Care and Use Committee (IACUC) at Boston Children's Hospital and followed the guidelines within the Association for Research in Vision and Ophthalmology (ARVO) Statement for the Use of Animals in Ophthalmic and Vision Research. The role of REV-ERBα in maintaining RPE health was evaluated in two genetically engineered mouse strains: a systemic knockout of REV-ERBα (*Rev-erbα*$^{-/-}$) strain and an RPE specific knockout of REV-ERBα (*BEST1-cre:Rev-erbα*$^{fl/fl}$) strain. Both strains are of C57BL/6J background and confirmed absence of *Crb1* (*rd8*) mutation by PCR to rule out potential confounding effects by *rd8* [77]. Generation of *Rev-erbα*$^{fl/fl}$ mice (provided by Dr. Laura Solt at the Scripps Research Institute) are described in detail in supplemental methods (Fig. S12). Two experimental models of RPE analysis were used: an RPE aging model and a chemical ($NaIO_3$)-induced RPE and retinal toxicity model. Fundus imaging and Optical Coherence Tomography (OCT) were used to monitor retinal morphology changes in live mice and *in vivo* images were taken from central retinas. RPE integrity and functions were examined with immunohistochemical staining in RPE/choroid/sclera flat mounts, and in eye cross-sections, as well as with electron microscopy. Histological images were random sampling of the whole retinas, except for when stated otherwise specifically. Histological changes and expression of biomarkers were assessed in sub-retinal regions of the eyes with both light and electron microscope imaging. Moreover, effects of activating REV-ERBα with small molecular agonists on protecting against sub-retinal damages were assessed in the chemical (NaIO3)-induced toxicity model *in vivo*. Primary mouse RPE cells were isolated from both *Rev-erbα*$^{+/+}$ and *Rev-erbα*$^{-/-}$ mice, and *in vitro* assays (phagocytosis, oxygen consumption, and cell viability) were performed in these cells to evaluate RPE health and functions. Transcriptional regulation of anti-oxidative enzyme system by REV-ERBα were evaluated in primary mouse RPE cells and ARPE-19 human RPE cell line with real-time qPCR, Western blot, ChIP and dual-luciferase reporter assay.

Detailed methods and materials are available in Supplemental Materials.

4.2. Statistics

All data were analyzed using GraphPad Prism version 8.0 (GraphPad Software, San Diego, CA). Sample sizes (n) for animals and/or eyes, and number of biological replicates for experiments are indicated directly in the figures or in the corresponding figure legends. Values shown in the graphs are presented as means ± SD of at least three independent experiments. Statistical differences between groups were analyzed using one-way analysis of variance (ANOVA) statistical tests, or two-way ANOVA, with appropriate post-hoc tests, or two-tailed unpaired *t* tests with unequal variance, unless stated otherwise in legends; P value $\leq$ 0.05 was considered statistically significant.

Funding

This work was supported by NIH/NEI R01 grants (EY031765, EY028100, and EY024963), BrightFocus Foundation, Research to Prevent Blindness Dolly Green Special Scholar Award, Boston Children's Hospital Ophthalmology Foundation, and Mass Lions Eye Research Fund Inc. (to J.C.). C.-H.L. and Z.W. acknowledge support by Knights Templar Eye Foundation Career Starter Grants.

Author contributions

S.H., C.-H.L. and J.C. conceived and designed the study; S.H. and J.C. wrote the manuscript. S. H., C.-H.L., Z.W., Z.F., W.R.B., and A.K.B. performed experiments and collected and analyzed the data; Z.F., T.M. K., J.L.D., and L.A.S. shared reagents and resources and provided expert advice; all authors edited and approved the manuscript.

Data and materials availability

The paper and the Supplementary Materials contain all methods and

data needed to evaluate the conclusions in the paper. Additional data and materials related to this study are available from the authors upon request.

One sentence summary

REV-ERBα regulates age-related retinal degeneration in RPE through transcriptional regulation of NRF2 and enhancing antioxidant defense.

Declaration of competing interest

The authors declare no financial interests/personal relationships which may be considered as potential competing interests.

Acknowledgments

We thank Drs. Lois Smith, Ye Sun, Yohei Tomita, and Bertan Cakir for helpful discussion.

Appendix A. Supplementary data

Supplementary data to this article can be found online at https://doi.org/10.1016/j.redox.2022.102261.

References

[1] P.T. de Jong, Age-related macular degeneration, N. Engl. J. Med. 355 (2006) 1474–1485.
[2] R.D. Jager, W.F. Mieler, J.W. Miller, Age-related macular degeneration, N. Engl. J. Med. 358 (2008) 2606–2617.
[3] L.S. Lim, P. Mitchell, J.M. Seddon, F.G. Holz, T.Y. Wong, Age-related macular degeneration, Lancet 379 (2012) 1728–1738.
[4] C. Bowes Rickman, S. Farsiu, C.A. Toth, M. Klingeborn, Dry age-related macular degeneration: mechanisms, therapeutic targets, and imaging, Investig. Ophthalmol. Vis. Sci. 54 (2013) ORSF68–80.
[5] R.F. Mullins, S.R. Russell, D.H. Anderson, G.S. Hageman, Drusen associated with aging and age-related macular degeneration contain proteins common to extracellular deposits associated with atherosclerosis, elastosis, amyloidosis, and dense deposit disease, Faseb. J. 14 (2000) 835–846.
[6] S. Umeda, et al., Molecular composition of drusen and possible involvement of anti-retinal autoimmunity in two different forms of macular degeneration in cynomolgus monkey (Macaca fascicularis), Faseb. J. 19 (2005) 1683–1685.
[7] J. Ambati, B.J. Fowler, Mechanisms of age-related macular degeneration, Neuron 75 (2012) 26–39.
[8] N.G. Lambert, et al., Risk factors and biomarkers of age-related macular degeneration, Prog. Retin. Eye Res. 54 (2016) 64–102.
[9] M. Mrowicka, et al., Analysis of antioxidative factors related to AMD risk development in the polish patients, Acta Ophthalmol. 95 (2017) 530–536.
[10] S. Datta, M. Cano, K. Ebrahimi, L. Wang, J.T. Handa, The impact of oxidative stress and inflammation on RPE degeneration in non-neovascular AMD, Prog. Retin. Eye Res. 60 (2017) 201–218.
[11] J.G. Hollyfield, et al., Oxidative damage-induced inflammation initiates age-related macular degeneration, Nat. Med. 14 (2008) 194–198.
[12] N. Wakabayashi, S.L. Slocum, J.J. Skoko, S. Shin, T.W. Kensler, When NRF2 talks, who's listening? Antioxidants Redox Signal. 13 (2010) 1649–1663.
[13] C. Tonelli, I.I.C. Chio, D.A. Tuveson, Transcriptional regulation by Nrf2, Antioxidants Redox Signal. 29 (2018) 1727–1745.
[14] H. Zhang, K.J.A. Davies, H.J. Forman, Oxidative stress response and Nrf2 signaling in aging, Free Radic. Biol. Med. 88 (2015) 314–336.
[15] L. Wang, et al., Nrf2 signaling modulates cigarette smoke-induced complement activation in retinal pigmented epithelial cells, Free Radic. Biol. Med. 70 (2014) 155–166.
[16] T. Rangasamy, et al., Genetic ablation of Nrf2 enhances susceptibility to cigarette smoke-induced emphysema in mice, J. Clin. Invest. 114 (2004) 1248–1259.
[17] Z. Zhao, et al., Age-related retinopathy in NRF2-deficient mice, PLoS One 6 (2011), e19456.
[18] F. van Asten, et al., A deep phenotype Association study reveals specific phenotype Associations with genetic variants in age-related macular degeneration: age-related eye disease study 2 (AREDS2) report No. 14, Ophthalmology 125 (2018) 559–568.
[19] G. Malek, Nuclear receptors as potential therapeutic targets for age-related macular degeneration, Adv. Exp. Med. Biol. 801 (2014) 317–321.
[20] G. Malek, E.M. Lad, Emerging roles for nuclear receptors in the pathogenesis of age-related macular degeneration, Cell. Mol. Life Sci. : CMLS 71 (2014) 4617–4636.
[21] M.A. Dwyer, D. Kazmin, P. Hu, D.P. McDonnell, G. Malek, Research resource: nuclear receptor atlas of human retinal pigment epithelial cells: potential relevance to age-related macular degeneration, Mol. Endocrinol. 25 (2011) 360–372.
[22] H. Migita, J. Morser, K. Kawai, Rev-erbalpha upregulates NF-kappaB-responsive genes in vascular smooth muscle cells, FEBS Lett. 561 (2004) 69–74.
[23] F. Guillaumond, H. Dardente, V. Giguere, N. Cermakian, Differential control of Bmal1 circadian transcription by REV-ERB and ROR nuclear receptors, J. Biol. Rhythm. 20 (2005) 391–403.
[24] H. Duez, et al., Regulation of bile acid synthesis by the nuclear receptor Rev-erbalpha, Gastroenterology 135 (2008) 689–698.
[25] N. Kumar, et al., Regulation of adipogenesis by natural and synthetic REV-ERB ligands, Endocrinology 151 (2010) 3015–3025.
[26] N.J. Mollema, et al., Nuclear receptor Rev-erb alpha (Nr1d1) functions in concert with Nr2e3 to regulate transcriptional networks in the retina, PLoS One 6 (2011), e17494.
[27] H. Cho, et al., Regulation of circadian behaviour and metabolism by REV-ERB-alpha and REV-ERB-beta, Nature 485 (2012) 123–127.
[28] E. Woldt, et al., Rev-erb-alpha modulates skeletal muscle oxidative capacity by regulating mitochondrial biogenesis and autophagy, Nat. Med. 19 (2013) 1039–1046.
[29] D.J. Kojetin, T.P. Burris, REV-ERB and ROR nuclear receptors as drug targets, Nat. Rev. Drug Discov. 13 (2014) 197–216.
[30] A.A. Butler, T.P. Burris, Segregation of clock and non-clock regulatory functions of REV-ERB, Cell Metabol. 22 (2015) 197–198.
[31] Z. Yang, et al., REV-ERBalpha activates C/EBP homologous protein to control small heterodimer partner-mediated oscillation of alcoholic fatty liver, Am. J. Pathol. 186 (2016) 2909–2920.
[32] M. Pariollaud, et al., Circadian clock component REV-ERBalpha controls homeostatic regulation of pulmonary inflammation, J. Clin. Invest. 128 (6) (2018) 2281–2296.
[33] M. Amir, et al., REV-ERBalpha regulates TH17 cell development and autoimmunity, Cell Rep. 25 (2018) 3733–3749 e3738.
[34] L.A. Solt, et al., Regulation of circadian behaviour and metabolism by synthetic REV-ERB agonists, Nature 485 (2012) 62–68.
[35] S. Raghuram, et al., Identification of heme as the ligand for the orphan nuclear receptors REV-ERBalpha and REV-ERBbeta, Nat. Struct. Mol. Biol. 14 (2007) 1207–1213.
[36] K.I. Pardee, et al., The structural basis of gas-responsive transcription by the human nuclear hormone receptor REV-ERBbeta, PLoS Biol. 7 (2009) e43.
[37] H. Duez, B. Staels, Rev-erb-alpha: an integrator of circadian rhythms and metabolism, J. Appl. Physiol. 107 (2009) 1972–1980, 1985.
[38] C. Crumbley, T.P. Burris, Direct regulation of CLOCK expression by REV-ERB, PLoS One 6 (2011), e17290.
[39] H. Cheng, et al., Photoreceptor-specific nuclear receptor NR2E3 functions as a transcriptional activator in rod photoreceptors, Hum. Mol. Genet. 13 (2004) 1563–1575.
[40] M. Chen, et al., Retinal pigment epithelial cell multinucleation in the aging eye - a mechanism to repair damage and maintain homoeostasis, Aging Cell 15 (2016) 436–445.
[41] G.S. Hageman, R.F. Mullins, S.R. Russell, L.V. Johnson, D.H. Anderson, Vitronectin is a constituent of ocular drusen and the vitronectin gene is expressed in human retinal pigmented epithelial cells, Faseb. J. 13 (1999) 477–484.
[42] J. Nguyen-Legros, D. Hicks, Renewal of photoreceptor outer segments and their phagocytosis by the retinal pigment epithelium, Int. Rev. Cytol. 196 (2000) 245–313.
[43] G. Inana, et al., RPE phagocytic function declines in age-related macular degeneration and is rescued by human umbilical tissue derived cells, J. Transl. Med. 16 (2018) 63.
[44] L.V. Johnson, G.S. Hageman, J.C. Blanks, Interphotoreceptor matrix domains ensheath vertebrate cone photoreceptor cells, Invest. Ophthalmol. Vis. Sci. 27 (1986) 129–135.
[45] F. Mazzoni, H. Safa, S.C. Finnemann, Understanding photoreceptor outer segment phagocytosis: use and utility of RPE cells in culture, Exp. Eye Res. 126 (2014) 51–60.
[46] P.K. Mukherjee, et al., Photoreceptor outer segment phagocytosis attenuates oxidative stress-induced apoptosis with concomitant neuroprotectin D1 synthesis, Proc. Natl. Acad. Sci. U. S. A. 104 (2007) 13158–13163.
[47] G. Yang, et al., Oxidative stress and inflammation modulate Rev-erbalpha signaling in the neonatal lung and affect circadian rhythmicity, Antioxidants Redox Signal. 21 (2014) 17–32.
[48] S. Sengupta, et al., The circadian gene Rev-erbalpha improves cellular bioenergetics and provides preconditioning for protection against oxidative stress, Free Radic. Biol. Med. 93 (2016) 177–189.
[49] T. Li, et al., Novel role of nuclear receptor Rev-erbalpha in hepatic stellate cell activation: potential therapeutic target for liver injury, Hepatology 59 (2014) 2383–2396.
[50] L.M. Franco, et al., Decreased visual function after patchy loss of retinal pigment epithelium induced by low-dose sodium iodate, Invest. Ophthalmol. Vis. Sci. 50 (2009) 4004–4010.
[51] H.M. Cocheme, M.P. Murphy, Complex I is the major site of mitochondrial superoxide production by paraquat, J. Biol. Chem. 283 (2008) 1786–1798.
[52] J. Cai, K.C. Nelson, M. Wu, P. Sternberg Jr., D.P. Jones, Oxidative damage and protection of the RPE, Prog. Retin. Eye Res. 19 (2000) 205–221.
[53] B. Dumas, et al., A new orphan member of the nuclear hormone receptor superfamily closely related to Rev-Erb, Mol. Endocrinol. 8 (1994) 996–1005.
[54] H.P. Harding, M.A. Lazar, The orphan receptor Rev-ErbA alpha activates transcription via a novel response element, Mol. Cell Biol. 13 (1993) 3113–3121.

[55] H.P. Harding, M.A. Lazar, The monomer-binding orphan receptor Rev-Erb represses transcription as a dimer on a novel direct repeat, Mol. Cell Biol. 15 (1995) 4791–4802.
[56] M.T. Lam, et al., Rev-Erbs repress macrophage gene expression by inhibiting enhancer-directed transcription, Nature 498 (2013) 511–515.
[57] G. Caratti, et al., REVERBa couples the circadian clock to hepatic glucocorticoid action, J. Clin. Invest. 128 (2018) 4454–4471.
[58] L. Yin, M.A. Lazar, The orphan nuclear receptor Rev-erbalpha recruits the N-CoR/histone deacetylase 3 corepressor to regulate the circadian Bmal1 gene, Mol. Endocrinol. 19 (2005) 1452–1459.
[59] D. Feng, et al., A circadian rhythm orchestrated by histone deacetylase 3 controls hepatic lipid metabolism, Science 331 (2011) 1315–1319.
[60] J. Iacovelli, et al., Generation of Cre transgenic mice with postnatal RPE-specific ocular expression, Invest. Ophthalmol. Vis. Sci. 52 (2011) 1378–1383.
[61] L. He, M. Marioutina, J.L. Dunaief, A.G. Marneros, Age- and gene-dosage-dependent cre-induced abnormalities in the retinal pigment epithelium, Am. J. Pathol. 184 (2014) 1660–1667.
[62] M. Teboul, F. Delaunay, [The orphan nuclear receptor Rev-erb alpha is a major component of the circadian clock], Med. Sci. 19 (2003) 411–413.
[63] S.N. Ramakrishnan, G.E. Muscat, The orphan Rev-erb nuclear receptors: a link between metabolism, circadian rhythm and inflammation? Nucl. Recept. Signal. 4 (2006) e009.
[64] A. Chawla, M.A. Lazar, Induction of Rev-ErbA alpha, an orphan receptor encoded on the opposite strand of the alpha-thyroid hormone receptor gene, during adipocyte differentiation, J. Biol. Chem. 268 (1993) 16265–16269.
[65] V.T. Vasu, C.E. Cross, K. Gohil, Nr1d1, an important circadian pathway regulatory gene, is suppressed by cigarette smoke in murine lungs, Integr. Cancer Ther. 8 (2009) 321–328.
[66] M.M. Olchawa, et al., Photosensitized oxidative stress to ARPE-19 cells decreases protein receptors that mediate photoreceptor outer segment phagocytosis, Invest. Ophthalmol. Vis. Sci. 54 (2013) 2276–2287.
[67] N. Aryan, B.S. Betts-Obregon, G. Perry, A.T. Tsin, Oxidative stress induces senescence in cultured RPE cells, Open Neurol. J. 10 (2016) 83–87.
[68] J. Hanus, et al., Induction of necrotic cell death by oxidative stress in retinal pigment epithelial cells, Cell Death Dis. 4 (2013) e965.
[69] Y. Imamura, et al., Drusen, choroidal neovascularization, and retinal pigment epithelium dysfunction in SOD1-deficient mice: a model of age-related macular degeneration, Proc. Natl. Acad. Sci. U. S. A. 103 (2006) 11282–11287.
[70] E.E. Brown, A.J. DeWeerd, C.J. Ildefonso, A.S. Lewin, J.D. Ash, Mitochondrial oxidative stress in the retinal pigment epithelium (RPE) led to metabolic dysfunction in both the RPE and retinal photoreceptors, Redox Biol. 24 (2019) 101201.
[71] H. Matsuoka, et al., Phosphoenolpyruvate carboxykinase, a key enzyme that controls blood glucose, is a target of retinoic acid receptor-related orphan receptor alpha, PLoS One 10 (2015), e0137955.
[72] L. Yin, et al., Rev-erbalpha, a heme sensor that coordinates metabolic and circadian pathways, Science 318 (2007) 1786–1789.
[73] Y. Zhang, et al., GENE REGULATION. Discrete functions of nuclear receptor Rev-erbalpha couple metabolism to the clock, Science 348 (2015) 1488–1492.
[74] A. Bugge, et al., Rev-erbalpha and Rev-erbbeta coordinately protect the circadian clock and normal metabolic function, Genes Dev. 26 (2012) 657–667.
[75] M. Surjit, et al., Widespread negative response elements mediate direct repression by agonist-liganded glucocorticoid receptor, Cell 145 (2011) 224–241.
[76] P. Dierickx, et al., SR9009 has REV-ERB-independent effects on cell proliferation and metabolism, Proc. Natl. Acad. Sci. U. S. A. 116 (2019) 12147–12152.
[77] M.J. Mattapallil, et al., The Rd8 mutation of the Crb1 gene is present in vendor lines of C57BL/6N mice and embryonic stem cells, and confounds ocular induced mutant phenotypes, Invest. Ophthalmol. Vis. Sci. 53 (2012) 2921–2927.